Ioannis Koutsamanis

Impact of storage conditions on the stability of hot-melt coated microcapsules containing lipid/emulsifier blends

MASTERARBEIT

zur Erlangung des akademischen Grades

Diplom-Ingenieur

Masterstudium Chemical and Pharmaceutical Engineering

eingereicht an der

Technischen Universität Graz

Betreuer

Univ. -Prof. Dr. Andreas Zimmer

Pharmazeutische Wissenschaften

Graz, November 2015

EIDESSTATTLICHE ERKLÄRUNG

AFFIDAVIT

Ich erkläre an Eides statt, dass ich die vorliegende Arbeit selbstständig verfasst, andere als die angegebenen Quellen/Hilfsmittel nicht benutzt, und die den benutzten Quellen wörtliche und inhaltlich entnommene Stellen als solche kenntlich gemacht habe. Das in TUGRAZonline hochgeladene Textdokument ist mit der vorliegenden Masterarbeit identisch.

I declare that I have authored this thesis independently, that I have not used other than the declared sources/resources, and that I have explicitly indicated all material which has been quoted either literally or by content from the sources used. The text document uploaded to TUGRAZonline is identical to the present master's thesis

Acknowledgements

First and foremost I would like to express my sincere gratitude to my supervisor Professor Andreas Zimmer and my second supervisor Dr. Sharareh Salar-Behzadi for the continuous support and guidance throughout this work as well as for their patience and engagement.

A special thank you goes to the PhD candidate Diogo Gomez Lopes for his insight, motivation, help with the equipment knowledge and for our long conversations during the last months.

Furthermore, I am grateful to Philipp Pernitsch, Viktoria Marko and the rest of the RCPE personal for their outstanding technical support.

I would like at this point to thank my parents for their constant support and encouragement and last but not least my partner Birgit Wanker and all my close friends for coping with my stress and keeping an open ear for me at all times.

Thank you!

Kurzzusammenfassung

In der pharmazeutischen Industrie gewinnen Lipide als Überzugshilfsstoffe an zunehmendem Interesse. Sie besitzen eine Vielzahl an Vorteilen, wie Geschmacksmaskierung, kontrollierten Wirkstofffreisetzung und biologische Abbaubarkeit.

Obwohl Studien zu Lipiden als Hilfsstoffe existieren, stellt sich die größte Herausforderung durch Ihren komplexen Polymorphismus, der sowohl einen Einfluss auf die Wirkstofffreisetzung als auch auf die Stabilität der Formulierung haben kann.

Vorangegangenen Studien haben gezeigt, dass die Verwendung von speziellen Emulgatoren in der Ummantelung sehr hilfreich sein kann; die Wirkstofffreisetzung kann auf diese Weise modifiziert werden und der Übergang in die nächste polymorphe Form wird entweder beschleunigt oder verlangsamt. Es existieren auch Studien, in denen über die Instabilität der Formulierung bei einer erhöhten Lagertemperatur berichtet wurde.

Das Ziel dieser Studie ist es, die Lagereigenschaften von Mikrosphären aus tripalmitin und Tween® 65, welche mittels ‚hot-melt fluid bed' Methode hergestellt wurden, in unterschiedlichen Konzentrationen und mit unterschiedlichen aktiven Kernkomponenten zu untersuchen.

Das Freisetzungsprofil der ummantelten Partikel wurde jeweils nach Ende der Produktion, nach einem Monat und nach drei Monaten Lagerung bei Raumtemperatur und bei 40°C analysiert.

Die Ergebnisse zeigen, dass die zwei verwendeten Komponenten des Partikelmantels mikroskopisch nicht mischbar sind. Die Löslichkeit des hydrophilen Emulgators in der Lipidphase ist so gering, dass sich eine Art 2-Phasen System bildet. So zeigt sich in der DSC Analyse, dass der Emulgator in der Ummantelung stets von dem Lipid getrennt ist. Im X-Ray Diffraction ist zu erkennen, dass es zu einem Wachstum der Lipidkristalle kommt, wenn diese bei 40°C gelagert werden. Bei dieser Temperatur ist der Emulgator jedoch geschmolzen. Die Unvermischbarkeit, die erhöhte Mobilität, die mit der Schmelzphase assoziiert ist, und das Wachstum der Lipidkristalle darauf hinweisen, dass die beiden Phasen stärker voneinander getrennt werden. Die Ansammlung des Emulgators ermöglicht es, dass Wasser leichter in die Mikrosphären penetrieren kann und sich daraus ein schnelleres Dissolutionsprofil ergibt

Abstract

Lipids as coating agents are gaining increased interest in the pharmaceutical industry. They possess a number of advantages such as test masking, controlled drug release and biodegradability.

Challenges arise however from the use of lipid excipients, the most important of which being their well-studied yet complicated polymorphism which has an impact on the formulation in terms of drug release and stability.

Previous studies showed that the addition of specific emulsifiers in the coating can be useful; the drug release can be furtherly modified and the transformation of one polymorphic form to the other can be either accelerated or hindered. Recent works reported however instability, when the formulation was stored at an elevated temperature.

The target of this thesis is to investigate the storage behavior of microcapsules produced with hot-melt fluid bed technology using tripalmitin as lipid and Tween® 65 as emulsifier in various concentrations and with different active cores.

The release profile of the coated particles was investigated after production, after one and three months of storage at room temperature and at 40°C. For the characterization of polymorphism and crystallite structure, differential scanning calorimetry (DSC) and X-Ray scattering were used.

The results indicate that the two components of the coating are microscopically immiscible. The solubility of the hydrophilic emulsifier in the lipid is very low creating a type of two-phase system. DSC results show that the emulsifier is always present separately while X-Ray diffraction indicates a growth of the lipid crystallites thickness when the samples are stored at 40°C. At this temperature, the emulsifier is melted. The immiscibility, the increased mobility associated with the molten state and the growth of the lipid crystallites could indicate that both phases are becoming more separated from each other. The accumulation of the emulsifier enables the water to penetrate the microcapsules easier resulting in a quicker dissolution profile.

Table of Contents

1 INTRODUCTION

The process of coating in the pharmaceutical industry is known since many decades. Various advantages such as drug protection, taste masking and modified drug release make the coating technology a widespread and much investigated process. Among the various equipment designed during the years, the development of the fluid bed technology is one of the most important achievements [1].

One variation of the fluid bed coating technology is the hot-melt coating. This solvent-free technique uses excipients that are brought to the molten state prior to the spraying and coating procedure. One group of these excipients that can be used for a solvent-free coating process is lipids and derivates of them [2]. Possessing a number of important advantages, lipid excipients are used more and more often for hot-melt coating. Polymorphism is however very often present in these compounds and can lead to various stability and drug release issues [3,4].

The effect of additives on the polymorphic crystallization of lipids has been already studied and indicates that various additives such as emulsifiers can inhibit or favor the quicker transformation of one polymorphic form to the other [5].

In a previous work, immediate release formulations were developed using tripalmitin and Tween® 65 as coating material. API crystals were hot melt coated with the coating material to provide microcapsule with immediate release in vitro performance. Tween® 65 was used in the formulation for two purposes: i) to induce the transformation of unstable alpha polymoph of tripalmitin to the most stable beta form, ensuring the storage stability, ii) to provide the immediate release profile of the encapsulated API, due to its relatively high HLB of 10.5 [6].

It has been however recently observed that after storage at elevated temperature, the microcapsules with the aforementioned coating formulation show a different dissolution profile. The stability of pharmaceutical products is of utmost importance for the industry and the development of new formulations. Stability tests include the storage of the sample in elevated temperature and/or humidity, exposure in light, oxygen and other environmental conditions.

The present work provides a mechanistic understanding of the above-mentioned unstable behavior of the coating formulation in elevated temperatures. Different active

pharmaceutical compounds were hot melt coated with tripalmitin and Tween® 65 in different ratios and coating amounts. The in vitro performance, and solid-state of coatings were analyzed after storage under different conditions.

This section provides a brief insight into the phenomenon of polymorphism in lipids, and describes the theoretical background of the various techniques used in this study.

2 THEORETICAL PART

2.1 Lipids and polymorphism

Triacyglycerols (TAGs) are the main constituents of edible oils and fats with other minor components being also present in this multi-component mixture. A triacylglycerol (TAG) molecule consist of three fatty acids esterified to a glycerol molecule. The general structure can be seen in Figure 1a.

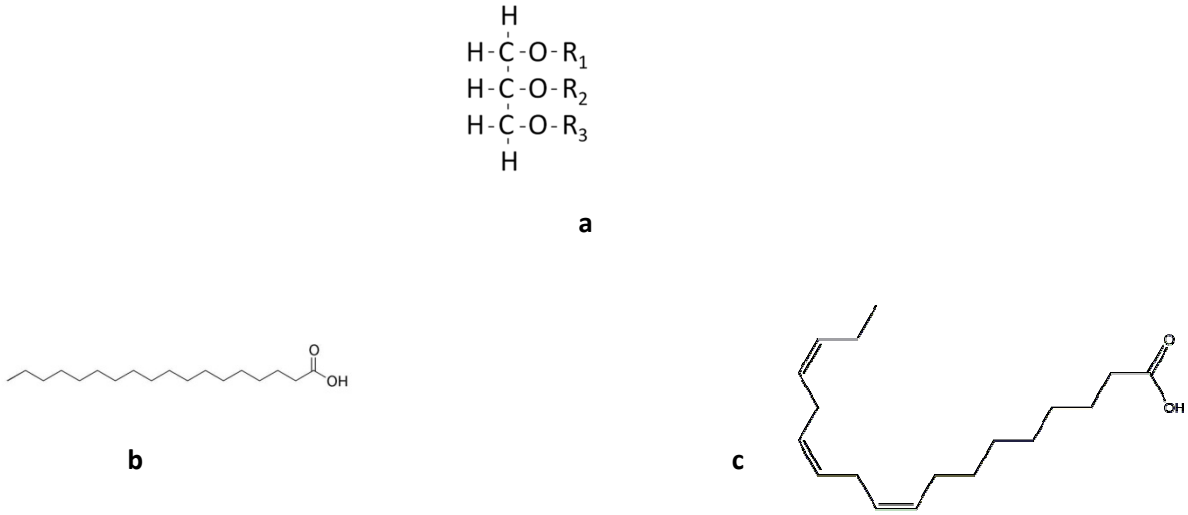

Figure 1. Chemical structures of (a) Triacylglycerol; (b) saturated fatty acid (stearic acid [37]**); (c) unsaturated fatty acid**

The three fatty acids can be the same (monoacid TAG: $R_1=R_2=R_3$) or different (mixed-acid TAG: $R_1\neq R_2\neq R_3$). The fatty acids themselves consist of a hydrocarbon chain with a number of 12-24 carbons in the chain being the most common. These chains can be saturated (Fig. 1b), unsaturated (Fig. 1c) or having a different stereochemical structure (cis-, trans-). With glycerol being always present in this structure, the composition of the fatty acids greatly influences the physical properties of the TAG [7].

Triglycerides exhibit a quite complex melting behavior and various crystalline forms. The three most common polymorphic forms existing are α, β´ and β, with α being the least and β the most stable form.

Like every specific polymorph type, these three forms show a characteristic carbon chain packing and thermal stability [8].

Because of the three long acyl chains the TAGs are orientated in a “chair” or tuning fork configuration in the crystalline lattice and they can have a double or triple chain-length structure as seen in Figure 2 [9].

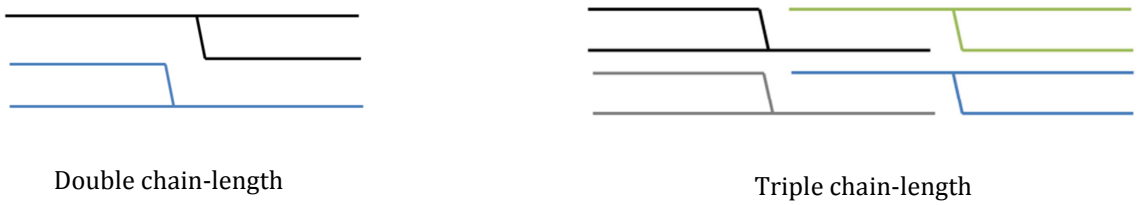

Figure 2. Chain length structure of triacylglycerides

The difference in the appearance of these configurations between polymorphic forms is mostly recognizable from the top view where the sub-cell configuration can be seen.

By using powder X-ray diffraction (XRD) crystallography, the subcell structures of the three polymorphic forms can be recognized: the diffraction patterns on the wide-angle XRD give information about the subcell structure which in other words are the distances between the acyl chains and the small-angle XRD gives information about the chain length packing which corresponds to the thickness of the TAG layer [7].

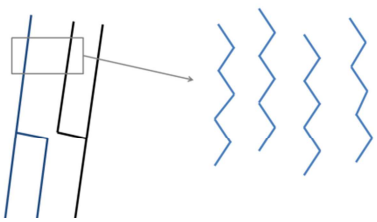

Figure 3. Chain length and subcell structure.

According to Gibb’s free energy the unstable form (α form) is the one to crystallize first [10].

Over time a transformation of the unstable to the more stable polymorphic forms will occur and this transformation can be also achieved by increasing the temperature slightly above the melting point of the unstable form. During this transformation the molecules become more tightly arranged in the crystal lattice.

The three common polymorphic forms present in the TAG structures are characterized from the sub cells that are found in the long chain alkyl molecules. These forms can be seen in Figure 4.

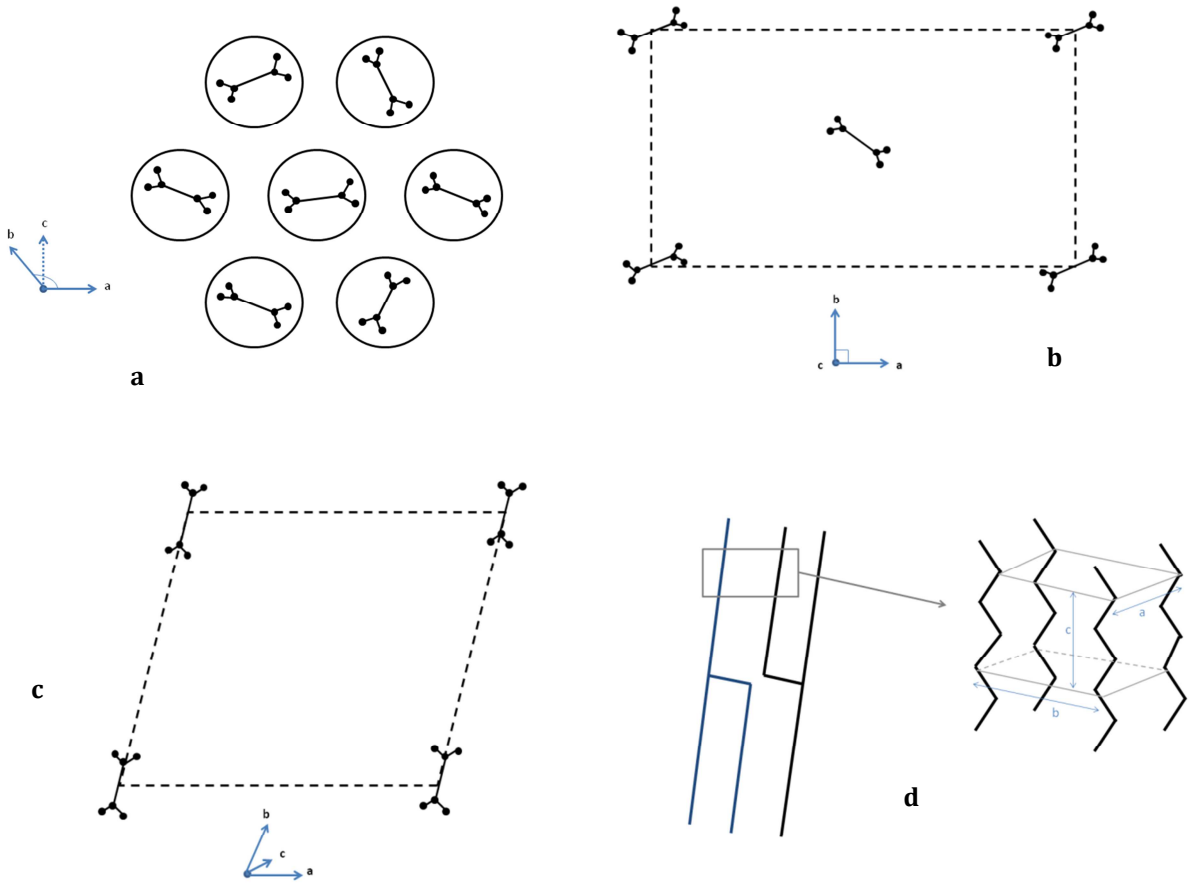

Figure 4. The common polymorphic forms of TAG (a) α-form; (b) β'-form; (c) β-form; (d) the subcell structure of TAG.

The α-form is characterized by the perpendicular to the figure arrangement of the hydrocarbon chains. Analyzing the diffraction patterns of that form, it is believed that this arrangement corresponds to the hexagonal packing of the chains. However, this form has not yet been completely defined and the analysis of the structure based on the diffraction pattern is considered to be quite unreliable [11].

The β'-form is represented by an orthorhombic packing of the hydrocarbon unit cells. The alkyl chains are, like in the case of the α-form, parallel to each other and perpendicular to the figure. One sub cell however is comprised by 5 instead of 6 chains.
The β-form is characterized by a triclinic packing of the sub cell units. The alkyl chains remain parallel to each other but the angle formed by the lattices is no more 90° as the chains are tilted and a unit cell is formed by 4 chain units.

Tripalmitin

Tripalmitin (Dynasan® 116) is a triglyceride consisting of three molecules of palmitic acid ($C_{16}H_{32}0_2$) esterified with one molecule of glycerol. Like the polymorphism of most fats, three main types are here encountered: α, β'and β. The melting point of each polymorph can be seen in the following table.

Polymorph type	Melting point (°C)*
α	45
β'	57
β	65

Table 1. Melting points of the polymorphic forms of Tripalmitin.

*Results according to the DSC thermograms of this study.

The molecular structures of these three polymorphic forms can be described as a disordered aliphatic conformation in alpha form, intermediate packing in beta prime and dense packing in beta form. Thus the Gibbs free energy has also the highest value in alpha, decreasing as we go to beta prime and beta [10].

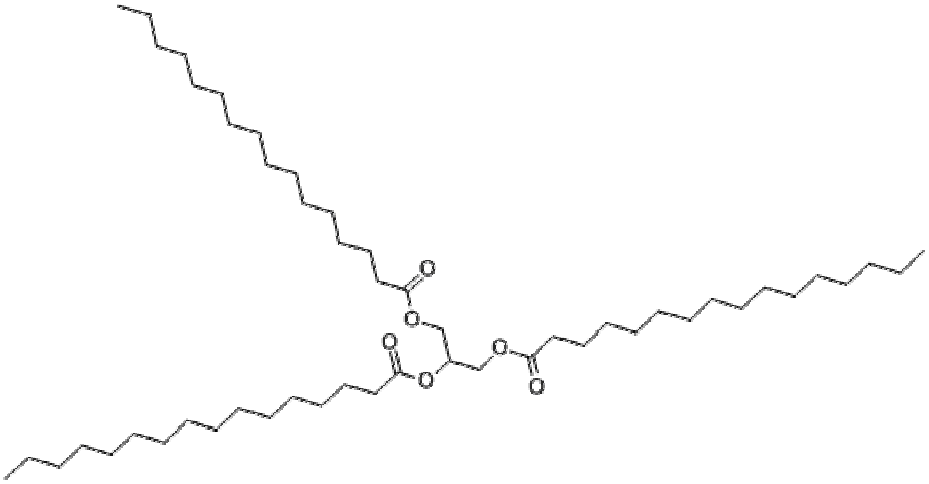

Figure 5. Chemical structure of Tripalmitin[38].

Tristearin

Tristearin (Dynasan® 118) consists analogously of three molecules of stearic acid ($C_{18}H_{36}O_2$) esterified with one molecule of glycerol. The polymorphism of tristearin is common to all TAG and also to that of tripalmitin. Again here there are three polymorphic forms α, β'and β with α the least and β the most stable form. The chain packing of the alpha form is hexagonal, that of beta prime orthorhombic and the packing of beta polymorphs forms a triclinic crystal lattice [12]. The melting points of each tristearin polymorph can be seen in the following table.

Polymorph type	Melting point (°C)*
α	57
β'	64,5
β	72

Table 2. Melting points of the polymorphic forms of Tristearin.

*Results according to the DSC thermograms of this study.

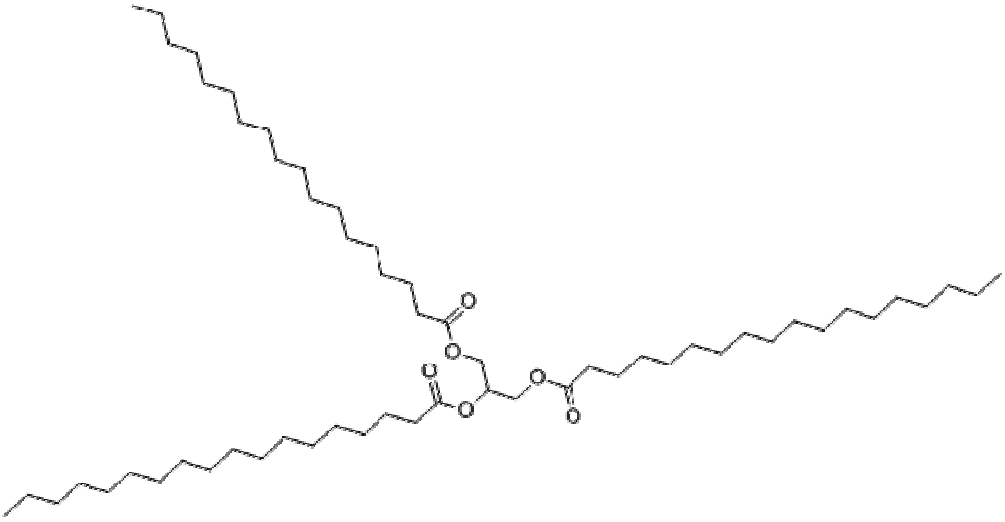

Figure 6. Chemical structure of Tristearin[39].

2.2 Manufacturing process

2.2.1 Coating technology

The process of coating in the pharmaceutical industry exists since more than 50 years. It is one of the most important and investigated manufacturing stages during the design and production of a pharmaceutical form.

Coatings in different forms are used to provide drug protection against exposure to environmental stress factors such as humidity, light and oxygen, taste masking, modified drug release, improve the aesthetic and appearance of the product, deliver the active compound in a form of "active coating", protect the mucosa from a possible irritation and for many more functions.

The instrumentation of coating technology includes various equipment such as rotating drums, pans, mixers and fluidized beds.

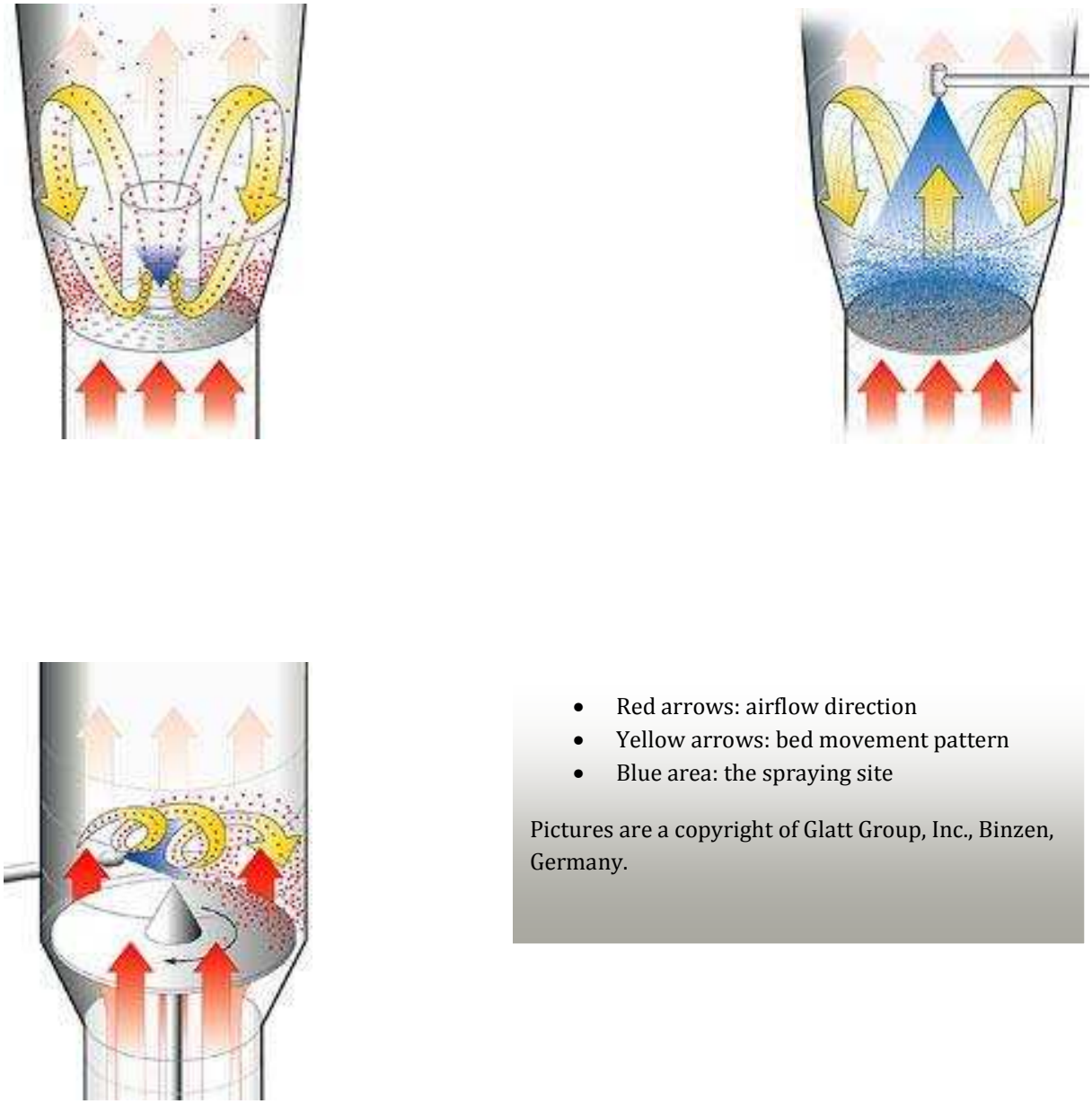

- Red arrows: airflow direction
- Yellow arrows: bed movement pattern
- Blue area: the spraying site

Figure 7. Fluid bed types; bottom spray, top spray and tangential spray.

Due to the importance of coating step in the manufacturing of pharmaceutical products, there is an ongoing improvement in the coating techniques, resulting in enhanced product quality, increased yield and reduced process time.

The inventions of the perforated pan and the fluid bed coater pointed to the right direction [13].

During the fluid bed process, the particle bed is fluidized with the help of airflow entering between the turntable and the chamber. The fluid bed keeps the particles in

that way in a fluidized state. There are three main types of fluid bed processors: bottom-spray (Wurster), top-spray and tangential spray (Figure 7*)*[1]. As the name indicates, the main difference between these fluid bed equipment is the site of spraying, with the spraying nozzle being respectively on the bottom of the product container, on the top spraying downwards or tangentially.

Fluid bed technology shows many advantages: the intensive mixing and the liquid-like particle movement in a fluidized bed results in a uniform temperature distribution, improves the solid and fluid contacting, enhances the heat and mass transfer resulting in a more even and smooth coating. Moreover the process can be performed continuous or batch-wise [14].
The fluid bed technique is widely used not only for the purpose of coating but also for granulation, drying and agglomeration processes [15].
By using a fluid bed coater the coating material prior to spraying is usually dissolved in an organic or water-based solvent. The evaporation of the solvent occurs during or after the coating process is finished[16].

Safety and environmental issues and the recovery of the solvents are however serious drawbacks that have turned the industry away of using organic solvents.
These disadvantaged have been overcome by the use of water or aqueous-based solvents.
However, the high enthalpy of water evaporation requires a slower drying process which increases the total process time. Apart from that, the risk of microbial contamination and the fact that some active compounds are instable in the presence of water have to be taken into consideration [2].
Solvent-free coating techniques receive more attention during the last years due to a number of advantages, the main of which *are:*

- Less energy input
- No time-consuming drying/solvent evaporation steps
- Much thicker coating can be obtained

[17]

Hot Melt Coating

Among the many solvent-free coating techniques developed, hot-melt is investigated as a coating process for pharmaceutical production since the end of the 2000s although this coating technique is known in food industry since decades. The coating material is applied on a molten state thus no solvent is required. Hot melt coating offers various advantages [18]:

- Avoidance of costly solvents, treatment or recovery of them as well as regulatory compliances
- Shorter process times-the coating agent is applied in a molten state
- No risk of hydrolysis and/or bacteriological contamination
- Effective taste masking and controlled release
- Easy modification from a conventional fluid bed coating apparatus
- According to their TD_{50}, lipids are often used for HMC and are considered as safe (Generally Considered As Safe-GRAS)

An overview of the most important part of the hot-melt coating equipment used in the present study (detailed information follows in the methods section) can be seen in the following figure (Figure 8, page 18).

The coating agent kept in a molten state is inside a container equipped with a normal or a magnetic stirrer (1). The bottom plate of the container is marked with (2), from which the hot air required for the fluidization of the particles is provided at a controlled temperature and pressure. The nozzle which provides the system with the molten coating agent is indicated in the center of the bottom plate (3). The spray rate, temperature of the nozzle and spray pressure can be as well controlled and monitored. Essential for the process are the filters (4) which capture the dust particles generated during the process.

1. Magnetic stirrer
2. Botttom plate
3. Nozzle
4. Filters

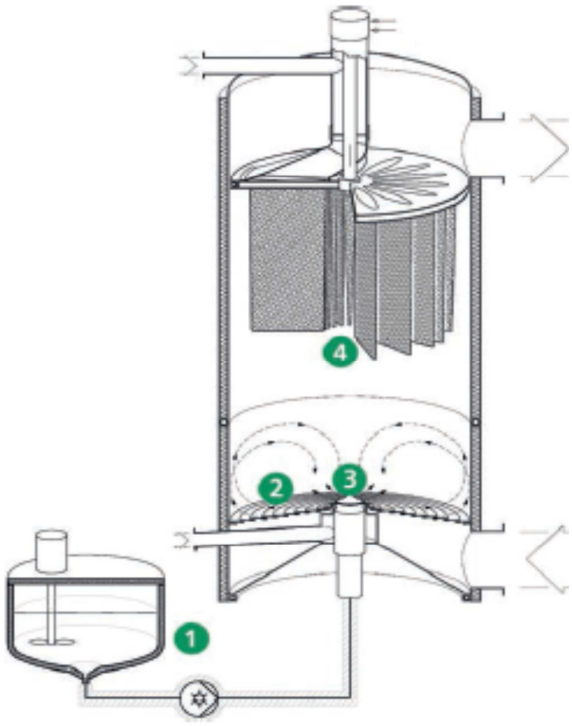

Figure 8. Hot-melt coating equipment schematic

In order to choose the appropriate lipid excipient as coating material, one has to consider several criteria: ability for taste masking, effect on the drug release profile, protection of the active compound and many physicochemical characteristics such as polymorphism, melting point and hydrophilic lipophilic balance (HLB). In the following table, examples of lipid excipients used in hot-melt coating can be seen [13].

Category	Chemical composition	Properties/ melting point	Function	Examples
Waxes	Esters of fatty acids and long chain alcohols	Hydrophobic/ 62-86°C	Prolonged release	Carnaube wax, beeswax
Vegetable oils	Triglycerides mixture, free fatty acids, phospholipids	Often digestible/ 60-71°C	Prolonged release and taste masking	Hydrogenated palm oil, hydrogenated cottonseed oil
Polyoxyglycerides	Mixture of glycerides, esters of fatty acids and PEG	Partially digestible/ ≈50°C	Prolonged or immediate release	Stearoyl polyoxyl-6 glycerides (Gelucire® 50/02)
Fatty acids	Long chain fatty acids	60-69°C	Prolonged release	Palmitic acid, stearic acid, behenic acid
Partial glycerides	Mixtures of mono-, di- and triglycerides	54-74°C	Prolonged release, lubrication, taste-masking	Glyceryl palmitostearate (Precirol® ATO 5), glyceryl monostearate (Myvaplex™ 600)
Animal fats	Clarified butter	≈80°C	Prolonged release	Cow ghee

Table 3. Lipid excipients used in hot-melt coating

2.3 Analytical methods - theory

2.3.1 Differential Scanning Calorimetry

Differential Scanning Calorimetry (DSC) is the most commonly used technique for analysis of the thermal properties of pharmaceuticals.
For the analysis, a sample (usually between 2-10mg) is placed in an aluminum crucible along with an empty reference pan in a furnace. Afterwards heating and/or cooling takes place at a controlled rate.

The principle behind, is that the thermodynamic response of the sample undergoing the thermal event will be measured and assessed in terms of heat flow and temperature. More specifically, it measures the enthalpy of a system by changing the temperature, based on the temperature difference between the sample and the reference, which is commonly air.

During a thermal event like melting or crystallization, the temperature and energy of this event are assessed. This information can be directly related to the solid-state structure of the sample.
Heating, cooling or an isothermal profile can take place by using a well specified heating/cooling rate program.

Although studying the melting profile of a sample has been the most common use of the technique for the pharmaceuticals, much more information can be obtained such as crystallization behavior, glass transitions and kinetic reactions [19]. This information is valuable for various areas of research such as quality control and identification of substances, stability and purity tests and characterization of samples in terms of crystallinity and kinetics.

There are two types of differential scanning calorimeters: heat flux DSC and power consumption DSC. Both have in common the fact that the measured signal is proportional to the heat flow rate φ and not simply heat [20].

Heat flux DSC

Heat flux DSC is the simpler of the two types and it is shown schematically in the following figure [19].

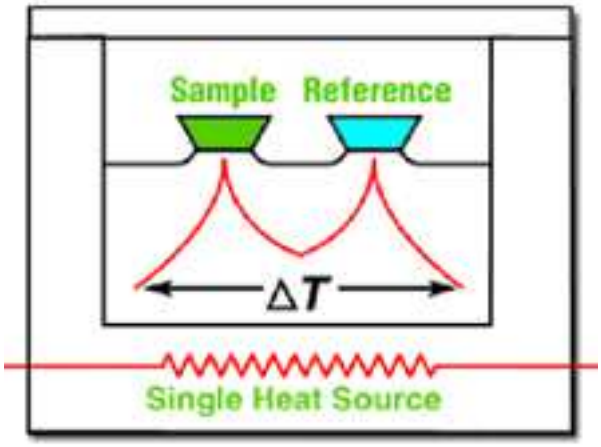

Figure 9. Heat flux DSC apparatus [40]

The two crucibles –one empty and the other containing the sample- are placed in a furnace with a thermocouple close to them. The two thermocouples are arranged back-to-back and the temperature difference is directly measured from the voltage developed from the thermocouples. The heat paths from the furnace to the sample and to the reference are identical and the equation for the heat flow from the furnace to each crucible is given by the following equation:

$$dQ/dt = \Delta T/R$$

Where Q=heat, t=time, ΔT=temperature difference between the furnace and the crucible and R=thermal resistance of the heat path between the furnace and the crucible.

From the previous equation, it is clear that the temperature difference between the sample and the reference is a measure of the difference in the heat flow due to the presence of the sample in only one of the crucibles [19]. In that way, this measurement of the heat flow is an indication of the properties of the sample and by having air as

reference, the heat losses, the absorption of heat by the reference material as well as other influences are eliminated.

Power compensation DSC

A power compensation DSC is shown in the following figure [19].

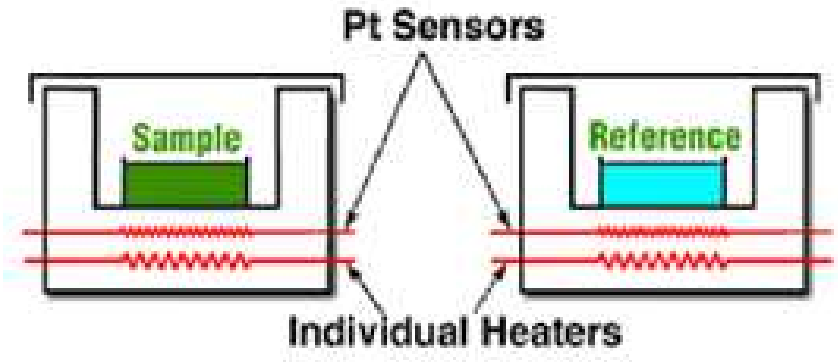

Figure 10. Power compensation DSC apparatus [40]

One obvious difference between this technique and the heat flux DSC is having two different furnaces -one for the reference and one for the sample. Both furnaces go through the same programmed temperature profile and the difference in power supplied to them is also here measured.

Another difference is programming the sample temperature and, in an ideal case, this should allow to have exactly the same temperature with the selected temperature profile.

Although the power compensation DSC should theoretically provide more accurate results, in practice both types of DSC analysis perform very similar in terms of sensitivity. A practical difference is that the fact that the power compensation DSC uses two small furnaces, these could achieve higher cooling and heating rates, which in some cases is desired.

2.3.2 X-ray scattering

General

Since the physicist and Nobel Prize laureate Max von Laue discovered in 1912, that crystalline materials act like diffraction gratings for X-ray wavelengths, x-ray diffraction is widely used for the characterization of crystal lattices and spacings.

The typical wavelength for x-rays is around 1 Å (0,1nm) and a common diffractometer uses copper x-ray tubes that produce x-rays with a wavelength of 1,54 Å. The size of the crystalline lattice which is also roughly around this wavelength of the x-rays makes it possible to use this scattering phenomenon for a thorough insight on the crystalline structure.

Figure 11 represents a geometrical description of the x-ray diffraction. As it can be seen on the figure, the incident x-rays hit the crystal plane at an angle θ. The x-rays normally penetrate the crystal to a certain depth, interacting with more than one parallel plane. Each plane striked by the x-ray will reflect some of the incident beam and the reflected ray will also create an angle θ.

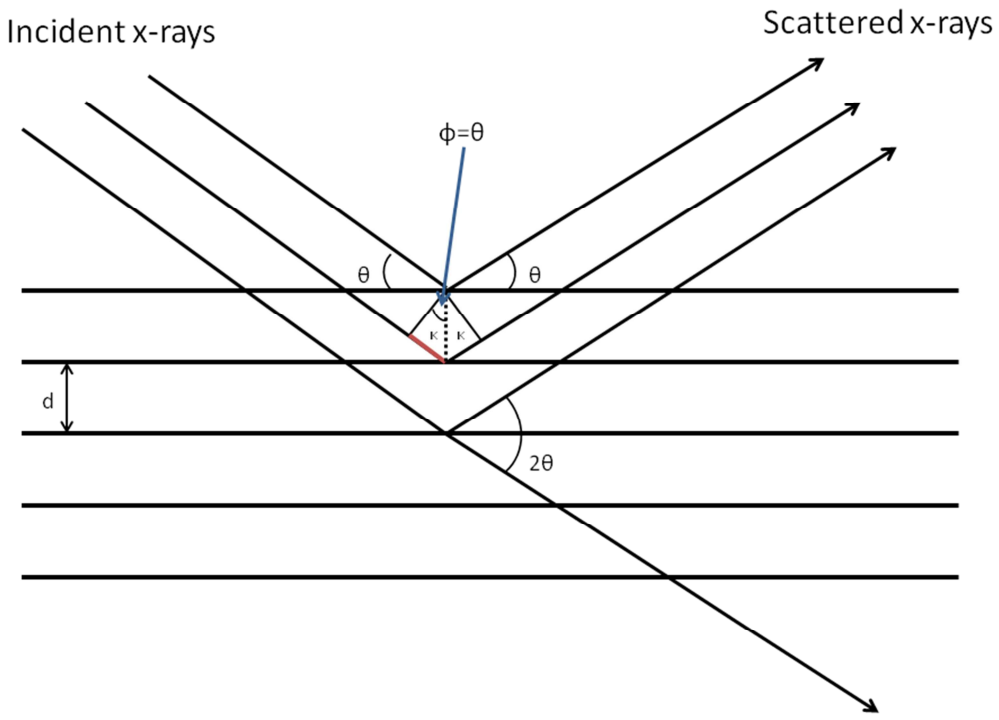

Figure 11. X-ray diffraction principle

The derived scattered x-rays interfere either destructively or constructively. Constructively means, that the difference in the distance, which the x-rays are traveling between planes, is equal to an integer number of wavelengths. Destructive interference means that this distance is not equal to an integer number of wavelength and when this is the case, no diffraction peaks can be seen.

It can be seen that the x-rays reflected on the second from the top plane travel an extra distance from the source to the detector. This extra distance is equal to 2κ (κ is indicated with red color on the sketch). According to the prerequisite for a constructive interference, this extra distance should be equal to:

$$\boldsymbol{n\lambda = 2\kappa}$$

Where n is an integer number and λ the wavelength of the incident x-rays.

If we want further to correlate the distance κ with the angle θ, we can see that:

$$\boldsymbol{\kappa = d \sin \theta}$$

Where d is the distance between the planes.

Each crystalline material has a unique x-ray powder diffraction pattern-this can be further used for the identification of that material. Relating the wavelength of the radiation to the diffraction angle and the space lattice in a crystalline sample one ends up with the Bragg's Law:

$$\boldsymbol{n\lambda = 2d \times sin\theta}$$

Scanning the sample through the full range of angles θ, all the diffraction directions of the beam are gathered, due to the random orientation of the powdered material. By converting the diffraction peaks to d-spacings one can identify the crystalline structure of the material [11,21].

Nanostructure characterization of fats and lipids

When triacylglycerol molecules crystallize, they take up a specific lattice arrangement and configuration. According to the definition of polymorphism, the molecules facilitate different ways of packing when arranging themselves in a crystal lattice. As mentioned before, triacylglycerols crystallize mainly into three different polymorphic forms; α, β' and β.
X-ray powder diffraction (XRD) is also in that case one of the most commonly used techniques for studying the crystal structure of lipids.

By using X-ray diffraction on fat crystals, two spacing types can be observed. Long spacings in the small angle region (1°-15°) and short spacings in the wide angle region of the pattern (16°-25°) (Figures 12-14) [20].
According to the structural network of fats the crystals are composed of nano-platelets, which consist of packed triacylglycerol molecules. TAG molecules packed together form a lamellae and several stacked lamellae form the nanoplatelets.

The long spacings (small angle X-ray scattering or SAXS) help identify the unit cells (Fig. 12) which corresponds to the thickness of the triacylglycerol layer and to the angle which forms because of the specific packing while the short spacings (wide angle X-ray scattering or WAXS) correlate to the cross-sectional packing of the unit cells (Fig. 13). This does not depend on the chain length. Using these two XRD peak intensities the different polymorphic forms of fats can be determined.

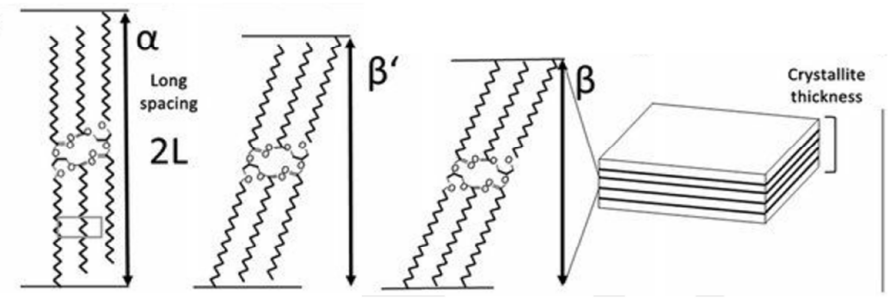

Figure 12. Long spacings of TAGs [32]

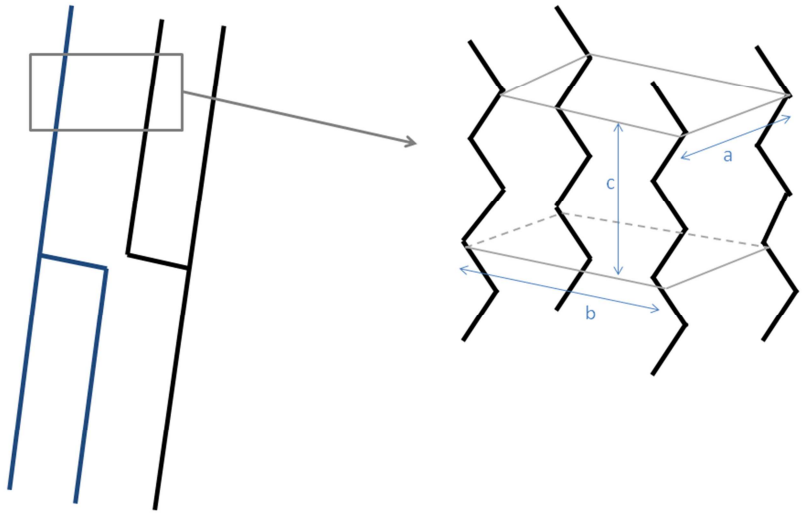

Figure 13. Short spacings of TAGs

The information acquired from the small angle region analysis can be furthermore evaluated using the Scherrer formula:

$$\boldsymbol{D = \frac{K\lambda}{FWHMcos(\theta)}}$$

Where λ Is the X-ray wavelength, FWHM (Full Width at Half Maximum) is the width in radians of the diffraction peak measured at half-way height when the intensity of the peak reaches $I_{max}/2$, θ is the diffraction angle and K is a dimensionless number shape factor with a typical value close to unity. Influenced by the shape of the crystal, it can vary from 0,62 to 2,08 with 0,9 being a good approximation in case of inadequate information [20].

Applying this formula, information about the average size of the crystallites can be extracted. It is however important to mention, that Scherrer's formula can be applied only for sized between 100-200 nm. Peak broadening is irreversible proportional to the crystallite size; this means a large crystal will induce a very sharp peak, the evaluation of which will be possibly subjected to errors, as it would be difficult to distinguish the

broadening of the crystallitk2e from the broadening caused by other factors, such as instrumental broadening [20].

Using Scherrer's formula, values for D are obtained which express the thickness of the nanoplatelets (Figure 14); and as explained earlier, these are the units formed by several TAG lamellae that are being stacked.

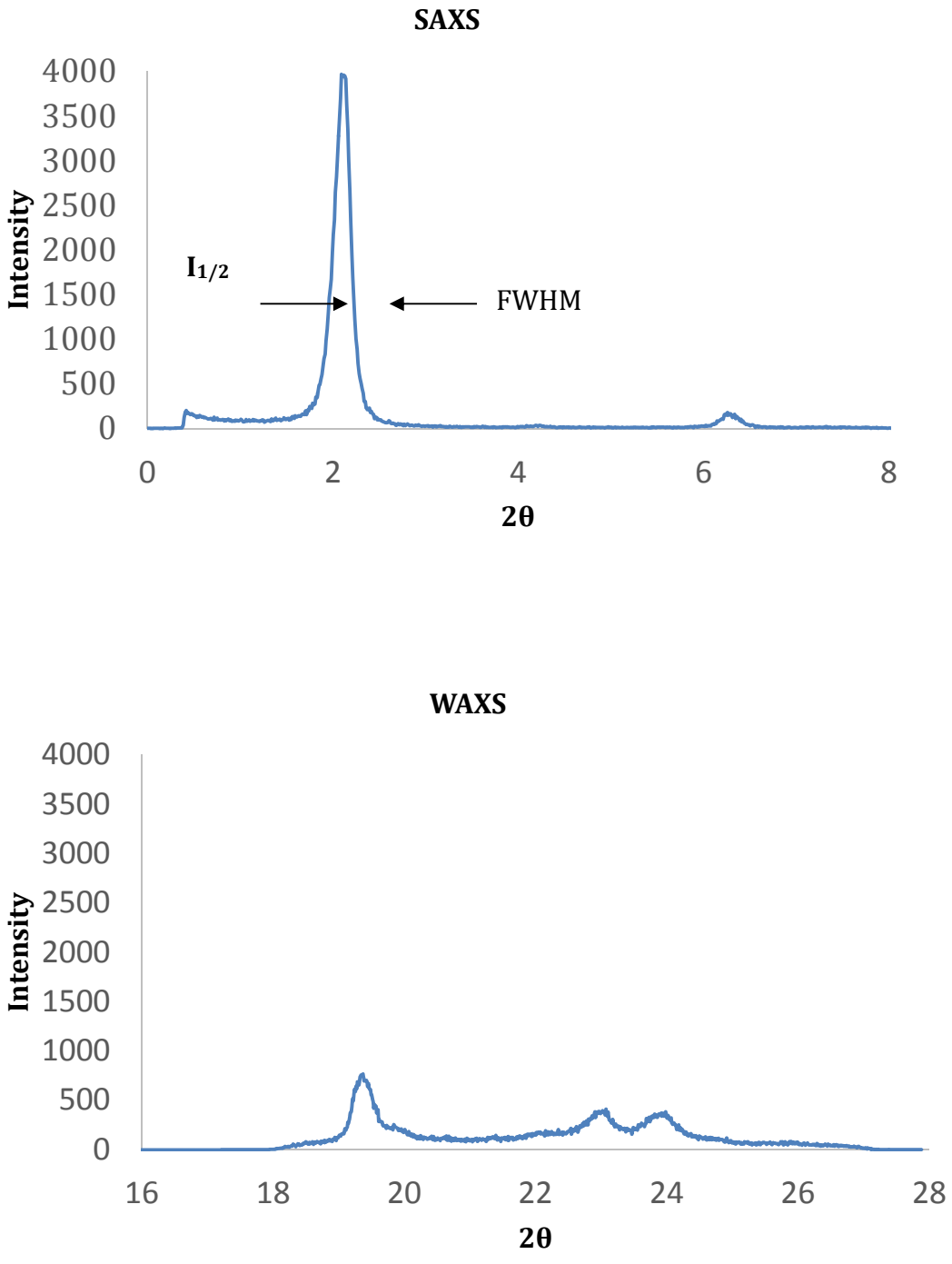

Figure 14. SAXS and WAXS diffraction peaks of N-Acetylcysteine microcapsules with 50% coating and 10% Tween® 65.

3 MATERIALS

3.1 Active Pharmaceutical Ingredients

3.1.1 N-Acetylcysteine

N-Acetylcysteine was provided by PharmaZell GmbH (Germany).

N-Acetylcysteine (from now on referred as 'NAc') (Fig.15a, MW=163.2 g/mol, $C_5H_9NO_3S$), is a derivate of L-cysteine with an acetyl group attached to the amino group (Figure 15). It appears as white or almost white, crystalline powder or colorless crystals. NAC is freely soluble in water and in ethanol (96%), practically insoluble in methylene chloride.

a **b**

Figure 15. (a) NAc; (b) L-cysteine

NAc is a prodrug to L-cysteine and it is converted to cysteine by the enzyme aminoacylase 1 (ACY1).

NAc is used for various indications and off-label uses with the two most common being:

- Mucolytic therapy – This the most common use of NAC. It splits the disulfide bonds of proteins that are present in the mucosa. This cause the reduction of the viscosity thus the easier expectorate of the mucosa.

- Paracetamol overdose – during a paracetamol induced overdose, the highly toxic metabolite NAPQI (N-Acetyl-p-benzoquinone imine) is accumulated. This metabolite is normaly conjugated by glutathione. When the glutathione reserves in the body are not

sufficient to deactivate NAPQI, this reacts with hepatic enzymes eventually damaging the liver. NAc is a glutathione component and helps replenish the levels of this enzyme in the organism [22–24].

In this study the NAc crystals were hot melt coated directly without any pre-processing to produce the microcapsules. The mean particle size of NAc (X_{50}) was found to be 527,31 +/-0,48 µm.

3.1.2 Ibuprofen sodium dihydrate

Ibuprofen Sodium was provided by BASF (Ludwigshaven am Rhein, Germany).

This salt derivate of Ibuprofen (Figure 16, $C_{13}H_{17}O_2Na$ x $2H_20$, MW: 228.26+36.03 g/mol) is highly water soluble (100mg/ml) and it appears as white crystalline powder. Ibuprofen is a propionic acid derivate and a well-known nonsteroidal anti-inflammatory drug (NSAID) with analgesic and antipyretic properties.

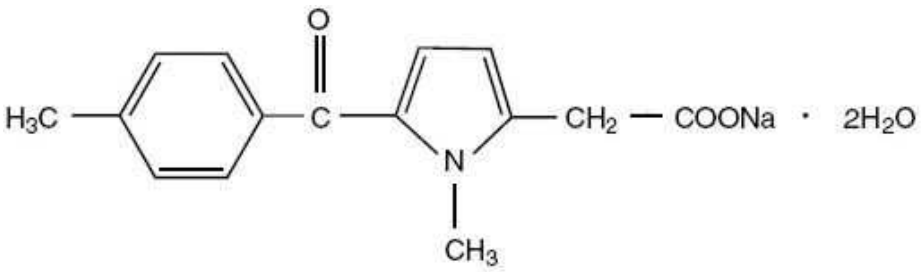

Figure 16. Ibuprofen sodium dihydrate [25]

Ibuprofen is used mainly against fever, mild-to-moderate pain, painful menstruation, osteoarthritis, dental pain and headaches and against inflammatory diseases such as rheumatoid arthritis.

The exact mechanism of action of ibuprofen is unknown. Ibuprofen is a non-selective inhibitor of cyclooxygenase (COX), an enzyme involved in prostaglandin synthesis.

It is believed that Ibuprofen inhibits cylooxygenase-2 (COX-2) which decreases the synthesis of prostaglandins involved in inflammation, pain and fever.

Being a non-selective agent, inhibiting also COX-1 is thought to cause some of the side effects of ibuprofen including GI ulceration.

Other effects include: nausea, dyspepsia, constipation, diarrhea, nosebleed, headache, dizziness, rash, and hypertension [22,25,26].

In this study, Ibuprofen sodium dihydrate was used as dry compacted granules. With a mean particle size X_{50} of 376,22 +/- 7,82 μm.

3.1.3 Citric Acid

Anhydrous citric acid was provided by Jungbunzlauer Swisse AG (Basel, Switzerland).

Citric acid (Figure 17, C6H8O7 MW=192.12 g/mol) is an organic acid found in citrus fruits and appears as a white, crystalline powder, colorless crystals or granules, very soluble in water, freely soluble in alcohol.

It is mainly used in the food industry as an acidifier, flavoring agent and preservative but its uses are expanded in the chemical industry (salts formation), cosmetics and other areas.

Like in the case of N-Ac, citric acid crystals were directly hot melt coated without any pre-processing to gain the microcapsules with an X50 of 796,74 +/- 22,63 μm.

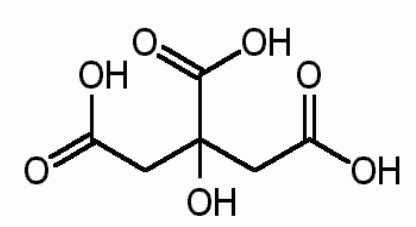

Figure 17. Citric acid [41]

3.2 Coating Agents

3.2.1 Tripalmitin

Tripalmitin (Dynasan 116® -Figure 18) is a white to almost white fine crystalline powder or flakes and was provided from CREMER Oleo Division (Witten, Germany).

Dynasans as brand names are different types of monoacid triacylglycerols: three fatty acids esterified with a glycerol molecule. They are approved from the FDA and are generally recognized as safe (GRAS).

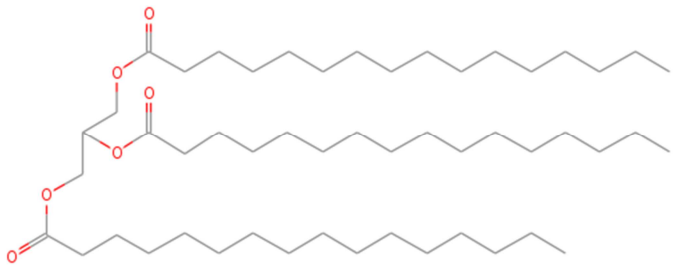

Figure 18. Tripalmitin (Dynasan 116®) [42]

3.2.2 Tween® 65

Tween® 65 was provided by Croda GmbH (Germany). Tweens® are oily substances (liquid or solid) which derivate when a sorbitan molecule gets PEG-ylated and then esterified with fatty acids.

Tween® 65 (Figure 19) is a yellow to light yellow solid substance with a melting point around 30-35°C [27–29]. According to the chemical structure description and IUPAC, Tween® 65 is also named Polyoxyethylene (20) sorbitan tristearate. The number 20 indicates the total number of oxyethylene -(CH_2CH_2O)- groups found in the molecule

(because of the PEG-ylation) and tristearate indicates that it has been esterified with three molecules of stearic acid.

Tween® 65 is known in the food industry as E 436. It is mostly used as a stabilisator, emulsifier and surfactant or wetting agent. Having an HLB factor of 10.5, it is considered an intermediate emulsifier, just over the barrier of 10 in this scale in order to be characterized as a hydrophilic emulsifier. According to its water solubility, it provides stable milky dispersions and can be used mainly as a W/O emulsifier.

As stated in the introduction, there are two reasons of using this specific emulsifier in the coating formulation. Firstly, the relatively high HLB value of Tween® 65 ensures an immediate release profile even at low concentrations. Secondly, it accelerates the transformation of the unstable α-form of tripalmitin to the stable β-form resulting in stable storage under room temperature conditions.

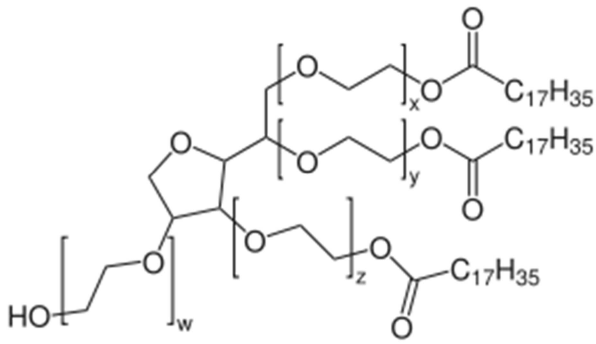

Figure 19. Tween® 65 [43]

4 METHODS

4.1 Hot-melt coating

4.1.1 Equipment

For the coating of the chosen pharmaceutical ingredients, a hot melt coating device (INNOJET HOTMELT DEVICE® IHD 1, Innojet Herbert Hüttlin E.k, Germany) was used which was connected with a laboratory-scale fluid bed equipment (INNOJET VENTILUS® IEV 2.5, Innojet Herbert Hüttlin E.k, Germany).

Figure 20. Hot-melt with fluid bed unit

Mixtures of tripalmitin and Tween® 65 with different ratios were used as coating formulations. In each hot-met coating run, the mixture of tripalmitin and Tween 65 is melted in a metal container under stirring and it is fed to the spray nozzle which is located in the bottom of the fluid bed container by a peristaltic pump (ISMATEC® IP65 Model ISM915A).

Along the silicon tube leading the molten mixture from the metal container to the spray nozzle, the temperature is kept constant over the melting point of the lipid/emulsifier mixture due to the unique design of the INNOJET HOTMELT DEVICE® IHD 1 equipment; the tubes containing the molten mixture are protected from temperature changes by being enclosed from special designed metal parts through which air with conditioned temperature flows.

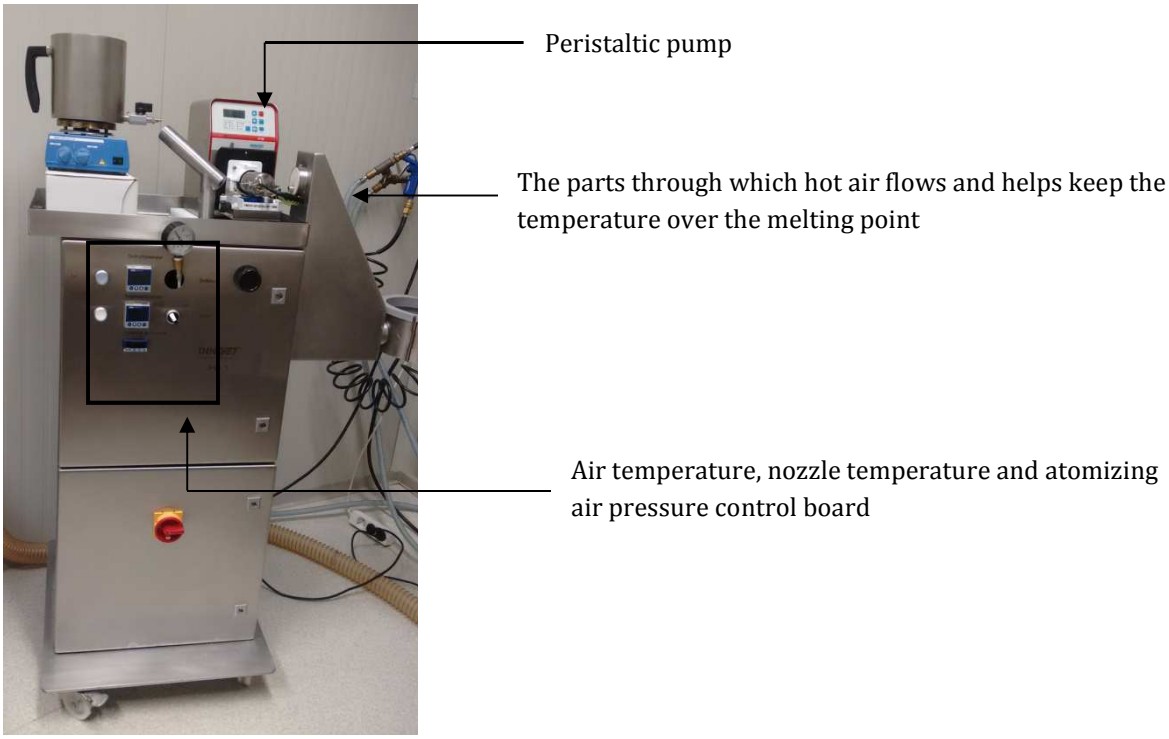

Figure 21. Hot-melt unit

The spray nozzle (INNOJET ROTOJET®) has also a specific design; it consists of three parts. The inner part provides the hot air to atomize the coating liquid while the outer part provides the molten mixture. The cylinder covering the outer part supplies the system also with so-called supporting hot air, to provide a certain spray angle. The bottom of the fluid bed container is equipped with INNOJET booster ORBITER®. This is a steel base plate comprised by overlapping parts; a perforated steel net and two circular

plates. This design of the guiding plates ensures a radial airflow which moves along the wall of the process container and then back to the center of the container [30].

Concerning the friable material and the dust generated during the process, the INNOJET SEPAJET filters are installed in the upper part of the fluid bed. These filters entrap the dust particles and the outlet air, free of dust, is recirculated back to the chamber. The whole process is controlled using a computer with the appropriate software provided by INNOJET Hüttlin, Germany.

a

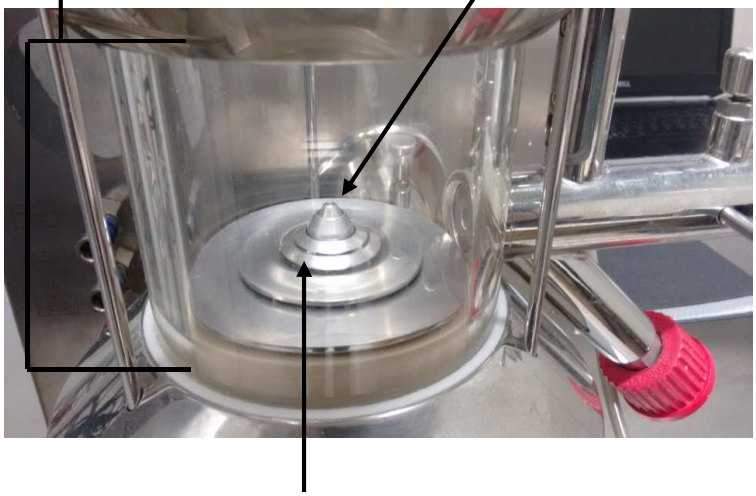

b

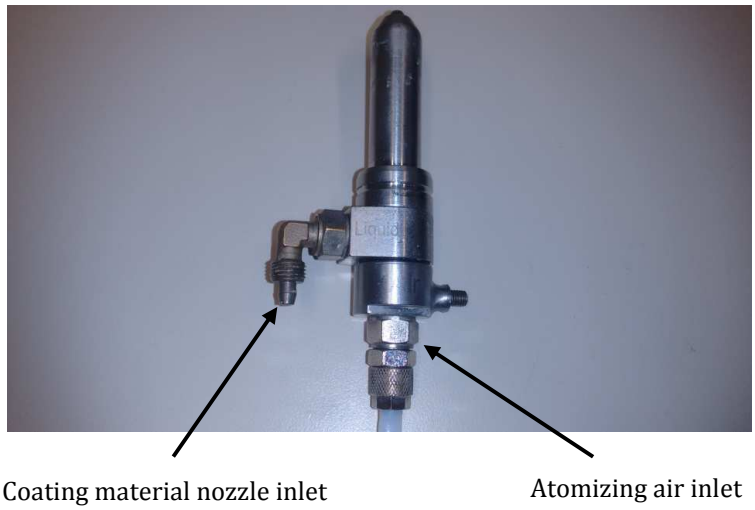

c

1: Inner part from where the hot spray air is provided
2: First outer part; coating liquid
3: Covering part; hot supporting air is provided

Figure 22. (a) 1L product container; (b) nozzle; (c) nozzle inner parts

4.1.2 Coating process

The lipid and emulsifier were in solid state in room temperature and were molten in a stainless steel container, constantly mixed using a magnetic stirrer during the whole coating process.
The temperature of the spray air as well as of the supporting air was kept at constant 100°C in order to ensure that the mixture is kept in a molten state.
Mounting of all the units was followed by ensuring the continuous flow of the coating material through the pipes and connections towards the spray nozzle. The whole system was afterwards sealed. The inlet temperature was adjusted to 25°C so that the coating formulation recrystallizes on the particles after a very short time of fluidization in the material container.
The batch of the selected pharmaceutical compound was fluidized in the fluid bed equipment by adjusting the inlet air flow to achieve a uniform fluidization of the particles. This flow of the particles before the actual spraying process starts ensures also the breakage of any aggregates formed during storage.
Once the particle bed reaches a steady flow, the atomizing air pressure is turned on and set to the desired level. Right after that step, the hot melt pump was activated and set to the spray rate desired. This step indicates the start of the coating process.

All the process parameters were held constant after that point and until the end of the process, with the exception of process air flow in a few cases.

During some coating procedures, which will be indicated later on, the process air had to be reduced due to high pressure difference on the SEPAJET filters, as a result of the high amount of dust generated and the long process needed in cases where a thicker coating was desired.
The following table provides an overview of the compositions and the parameters used during the hot melt coating process.

4.1.3 Compositions and parameters

API	Coating Amount (%)	Tripalmitin/ Tween® 65 ratio in coating (%)	Spray rate (rpm/g·min^{-1})*	Spray pressure (bar)	Inlet temperature (°C)	Process air (m^3/h)	Batch number	API batch size (g)
NAc	50	90/10	50/7.2	1,1	25	50**	1404151	300
NAc	50	70/30	50/7.2	1,1	25	50**	1404152	300
NAc	70	90/10	50/7.2	1,1	25	35	1805152	250
NAc	70	70/30	50/7.2	1,1	25	35	1805151	250
Ibuprofen Sod. Dih.	50	90/10	50/7.2	1,1	25	30	2904152	300
Ibuprofen Sod. Dih.	50	70/30	50/7.2	1,1	25	30	2904151	300
Ibuprofen Sod. Dih.	70	90/10	50/7.2	1,1	25	30	3004152	180
Ibuprofen Sod. Dih.	70	70/30	50/7.2	1,1	25	30***	3004151	180
Citric acid	50	90/10	50/7.2	1,1	25	35****	0605151	200
Citric acid	50	70/30	50/7.2	1,1	25	35****	2204152	200
Citric acid	70	90/10	50/7.2	1,1	25	45*****	0705152	200
Citric acid	70	70/30	50/7.2	1,1	25	45	0705151	200

* During the first 5' of the coating process, the following spraying rate schema took place:

Minute of process	Spray rate (rpm)
0-2'	35
2-4'	40
4-5'	45
5'-end	50

Table 4. Hot-melt coated microcapsules composition and manufacturing parameters

4.2 Analytical methods

4.2.1 Dissolution tests

For the investigation of the dissolution profile, a dissolution tester with autosampler (Erweka dissolution tester DT 820-USP Apparatus 2) was used.
All samples were tested right after production (t0), as well as after one and after three months storage under two different conditions; room temperature and 40°C.

The conditions for the dissolution tests can be seen in table 5.

Dissolution tester	Erweka dissolution tester DT 820 with autosampler
RPM	100
Agitation	USP type 2 - paddles
Dissolution medium	Phosphoric Buffer (pH 6,8 ±2%)
Volume (ml)	900
Medium temperature (°C)	37±0,5
Sampling points (min)	Baseline (0), 1, 5, 10, 15, 20, 30, 45, 60, 90
Sample volume (ml)	1,5

Table 5. Dissolution tests conditions.

After warming up the medium in the dissolution vessels, the baseline was withdrawn. Then the amount of microcapsules equal to a single dose of each pharmaceutical compound was added to the vessels and the test was started.

Compound	Single dose (pure compound in mg)	Single dose (cores of compounds in mg)
N-Acetylcysteine	600	600
Ibuprofen Sodium dihydrate	512.5 (equivalent to 400 mg of Ibuprofen free acid)	545.2
Citric acid	500	500

Table 6. Single-dose per API.

From the previous table, it can be observed that although in the cases of NAc and citric acid, the compounds were used as pure cores for the coating process, there is an exception in the case of Ibuprofen Sodium. Ibuprofen Sodium dihydrate has to go through a granulation process prior to coating because of the physical properties of the compound. Being powder-like dusty material it is impossible to undergo a coating procedure without a granulation step. In our case, dry granulation was implemented using a roll compactor (Alexanderwerk WP120 Pharma, Alexanderwerk, Germany).

The granules of Ibuprofen Sodium produced have the following composition and physical characteristics.

Active compound	Ibuprofen Sodium dihydrate
Excipients (% w/w)	2,5 Sorbitol (Parteck SI 150) 3,5 Isomalt (GalenlQ 721)
Friability (% w/w)	52,5
Bulk density	0,543 mg/ml

Table 7. Ibuprofen sodium dihydrate granules composition and physical properties.

For the reference solutions, the pure compounds were used and dissolved into the dissolution medium.
The reference solutions were made for 25, 50, 70, 100 and 130% of the concentration in the dissolution vessels (single-dose in 900ml of medium).

In order to compare the different dissolution profiles, the similarity factor (f2) was used which is defined as [31]:

$$f2 = 50 \times \log\left\{\left[1 + \left({}^{1}/_{n}\right)\sum (Rt - Tt)^2\right]^{-0,5} \times 100\right\}$$

Where:

n= number of time points

Rt= dissolution value of the reference batch at time t

Tt= dissolution value of the test batch at time t

When two dissolution profiles are completely identical, the f2 value is equal to 100. Generally, f2 values between 50 and 100 are considered to be similar.

4.2.2 Content assay

The coated microcapsules were evaluated in terms of content by first cryomilling and then dissolving of the extracted API in a buffer solution. The coated particles were cooled with nitrogen down to -196° C and subsequently grinded in a cryomill (Retsch Haan, Germany) for two circles at 25 Hz.

The cryomilled samples were then dissolved in 100 ml medium, the solutions were put in an ultrasonic bath and were intensively shaken every 2-3' for 1'. A filtration step followed, using 0,45μm pore filters (Yeti Nylon Syringe Filters, 0.45 μm, 25 mm, Merz Brothers GmbH, Haid, Asutria) and 1ml of each filtrated solution was diluted with 9ml of Phosphoric Buffer.

The last step included a filtration with HPLC compatible filters (Yeti 0,22 μm MCE syringe filters, Merz Brothers, Haid, Austria) and the final dilutions were analyzed using HPLC (Waters 2996 PDA Detector HPLC system, Waters Corporation, Milford, USA).

The next table summarizes the media and conditions implemented for microcapsules containing each active compound.

Active compound	First step medium	Ultrasonic bath
NAc	Phosphoric buffer (pH 6,8)	15' at room temperature
Ibuprofen Sodium dihydrate	0,1 KOH solution (pH 12,8)	10' at 50°C
Citric acid	Phosphoric buffer (pH 6,8)	15' at room temperature

Table 8. Content assay conditions per API.

The HPLC methods used for the evaluation of each API's concentration are summarized in the following table.

Active compound	Citric acid	N-Acetylcysteine	Ibuprofen
Column	PurospherStar (Merck), RP-18e (5µm), Hibar RT 150-4,6 with pre-column	PurospherStar (Merck), RP-18e (5µm), Hibar RT 150-4,6 with pre-column	PurospherStar (Merck), RP-18e (5µm), Hibar RT 125-4 with pre-column
Flow (ml/min)	1	1	1
Wavelength (nm)	215	220	231
Column temperature (°C)	25	21	21
Probes temperature (°C)	5	5	5
Injection volume (µl)	20	20	20
Run time (min)	7 (peak: 5)	12 (peak: 4,5)	10 (peak: 3,8)
Mobile phase	0,01 mol/L KH_2PO_4 (pH 2,2 with H_3PO_4)	95% H_2O / 5% ACN (pH 1,6 with H_3PO_4)	67% ACN / 33% H_2O + 5ml 8,5% H_3PO_4
Rinsing solution	70 ACN / 30 H_2O	H2O	70 ACN / 30 H_2O
Comments		Storage at 4°C to avoid degradation	

Table 9. HPLC methods implemented for each active compound.

4.2.3 Differential Scanning Calorimetry

Samples preparation

Various physical mixtures of tripalmitin and tristearin with Tween® 65 as well as the reference materials (pure tripalmitin, tristearin and Tween® 65) were prepared by weighing the compounds using an analytical balance inside beaker glasses.
The mixtures were molten and stirred for 5' with a magnetic stirrer for homogenization, prior to the preparation of the DSC crucibles.
Mass between 2-3mg was placed in the crucibles using an Eppendorf pipette. The lids were perforated and the crucibles were sealed afterwards. The pans are made of Aluminum and are ordered from NETZSCH GmbH, Selb, Germany. Triplicates of the samples for immediate (time 0) measurement as well as for one and three month storage were prepared. The storage conditions chosen were both room temperature and 40°C inside a drying chamber.

The following table sums up the ratios of mixtures prepared for the DSC measurements.

Lipid	Tripalmitin			Tristearin		
Time	t0	1M	3M	t0	1M	3M
Tween® 65 amount (% w/w)	0	0	0	0	0	0
	10	10	10	10	10	10
	25	25	25	25	25	25
	50	50	50	50	50	50
	75	75	75	75	75	75
	100	100	100	100	100	100

Table 10. Blends prepared for DSC analysis.

Implementation

The differential scanning calorimeter used was a DSC 204 F1 Phoenix, (NETZSCH GmbH, Selb, Germany).

The next table summarizes the heating/cooling program that was chosen for the measurements.

Mixture	Starting point (°C)	Heating Rate (°C/min)	Endpoint (°C)	Cooling Rate (°C/min)	Endpoint (°C)
Tripalmitin/ Tween® 65	-20	2	90	2	-20
Tristearin/ Tween® 65	-20	5	90	10	-20

Table 11. DSC heating/cooling programs.

4.2.4 X-ray scattering

For the x-ray measurements, a SWAXS compact Kratky camera with line-focus optics (HECUS X-ray Systems, Graz, Austria) mounted on a sealed-tube X-ray generator (Seifert, Ahrensburg ,Germany) operating at 30kV and 0.4mA was used. CuKa radiation was used with a wavelength of λ=1.542˚A and the angular range was 0,06°<2θ>8°. Samples of each microcapsule after storage under 2 different conditions; room temperature and 40°C were placed in a glass capillary with a diameter of approximately 2mm, which was later sealed with wax and placed into the capillary rotation unit. The measurements were performed in triplicates, at room temperature with an X-ray exposure time of 1200s [32].

4.2.5 Particle Size Distribution

For the particle size analysis, a high speed picture analysis sensor QICPIC (Sympatec GmbH, Clausthal-Zellerfeld, Germany) equipped with a RODOS/L dry dispersion unit was used.

The injector used has a diameter of 4mm, the primary pressure to disperse the particles was 0,5bar and the frame rate 400Hz (frames/second). As a unit for the measured particles, the equivalent diameter of the circle with the equal projection area with the particle was chosen (EQPC).

In order to acquire a full overview of the produced microcapsules, all the samples were measured after the coating process as well as the three pure compounds; citric acid, NAc crystals and Ibuprofen sodium dihydrate granules.

5 RESULTS

5.1 Dissolution profiles

5.1.1 N-Acetylcystein

The following figures (Fig. 23-26) show the release profile of the microcapsules containing NAc.

Figures 23 and 24 show the samples with 50% of coating amount (10% and 30% of Tween® 65).

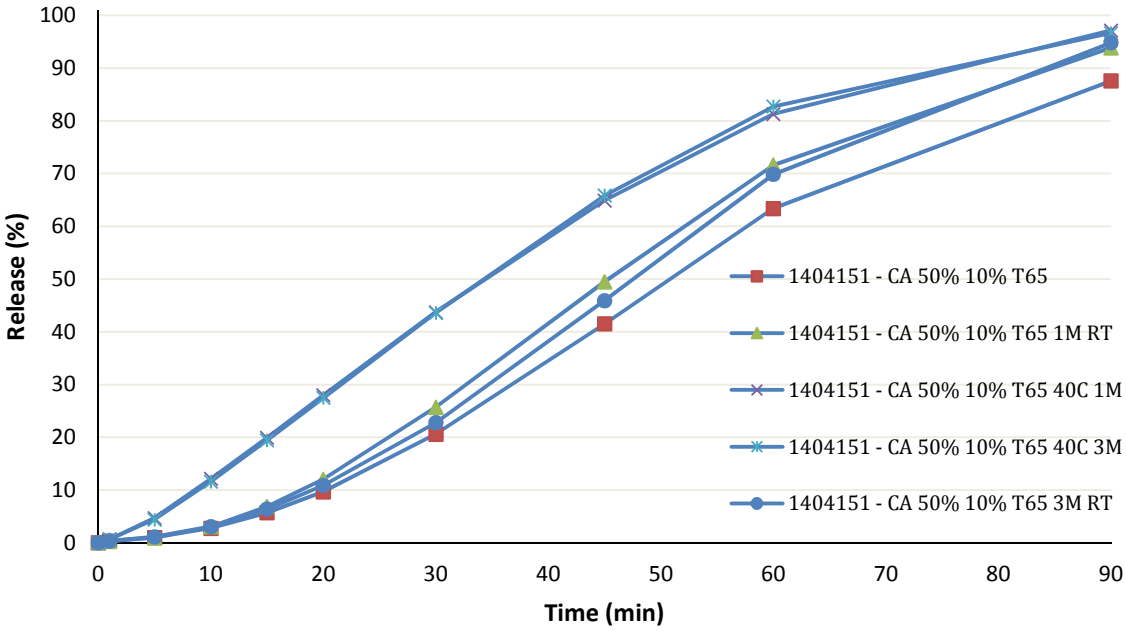

Figure 23. Dissolution profile of NAc microcapsules containing 50% coating and 10% Tween® 65

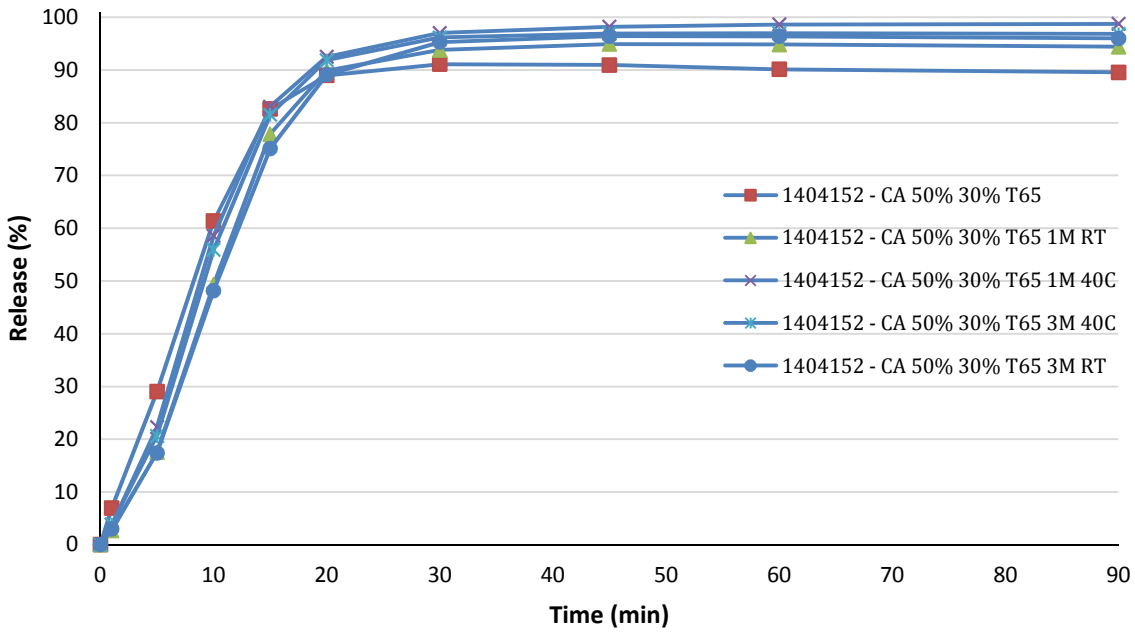

Figure 24. Dissolution profile of NAc microcapsules containing 50% coating and 30% Tween® 65

Figures 25 and 26 show the samples with 70% of coating amount (10% and 30% of Tween® 65).

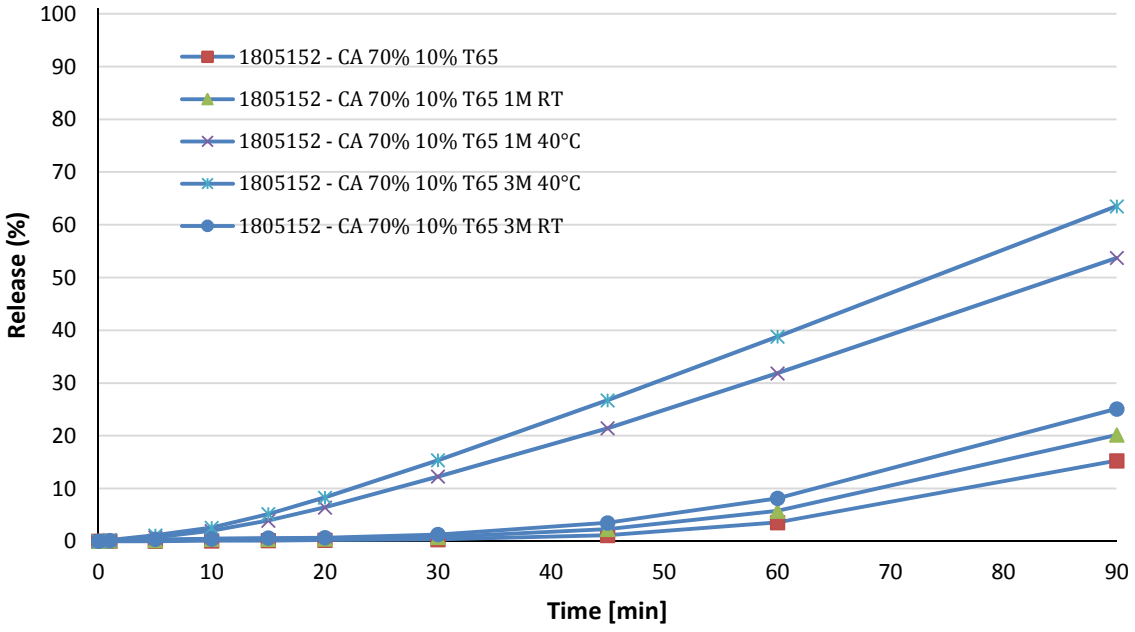

Figure 25. Dissolution profile of NAc microcapsules containing 70% coating and 10% Tween® 65

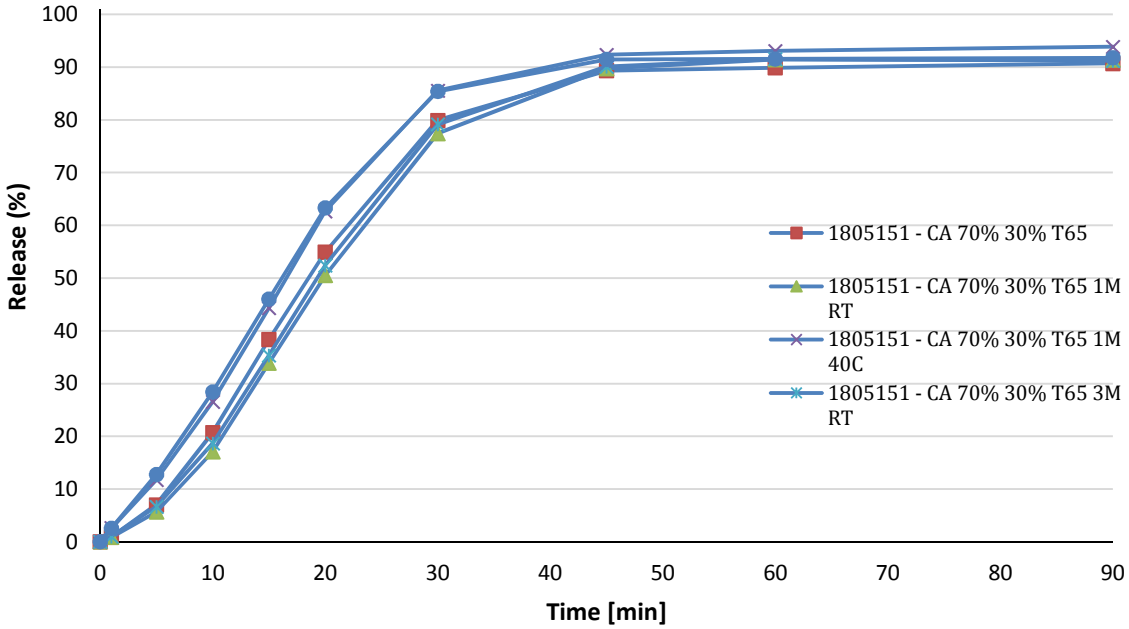

Figure 26. Dissolution profile of NAc microcapsules containing 70% coating and 30% Tween® 65

The dissolution profile of NAc with the 50% coating amount and 10% of the emulsifier (Fig. 23) is significantly increased after storage in 40°C for one month (f2=40). This is not the case after storage in room temperature for the same time (f2=66). The dissolution profiles of the formulation after 3 months of storage remain almost identical compared with the ones after 1 month (f2=96 for 40°C storage, f2=85 for room temperature).

Taking a look at the dissolution profiles of the formulation with the same coating amount but with 30% emulsifier content, it is obvious that the profiles are identical with all comparisons between them yielding an f2 between 56 and 88.

The same behavior can be observed in the formulations consisting of 70% coating (Figures 25, 26).

The microcapsules with 10% emulsifier show a clearly faster release after storage for 1 month in 40°C with a f2=37 in comparison to a f2=84 for the formulations stored for one month in room temperature. Comparing the stored formulations, showed a faster but not significantly different dissolution profile (f2=84 between one and three months storage in room temperature and f2=67 in 40°C).

Having 30% emulsifier in that system, the release profile of NAc after production was comparable with the release of API from samples stored under different conditions ($55 \leq f2 \geq 90$).

The significantly accelerated release of NAc from microcapsules containing 10% Tween® 65 after storage in 40°C might be related to the phase separation between lipid and emulsifier. This is due to the relative low melting point of Tween® 65 (31~34°C according to the DSC results present on this study). By increased amounts of Tween® 65 in the coating (30% w/w), the release will not be significantly affected, because of the easier penetration of the aqueous medium in the microcapsules, due to the relative high HLB value (10,5) of this emulsifier.

5.1.2 Ibuprofen sodium dihydrate

The following figures (27-30) present the release profiles of the microcapsules containing Ibuprofen sodium dihydrate.

More specifically, figures 27 and 28 show the release of the samples with 50% of coating amount (10% and 30% of Tween® 65 in the coating).

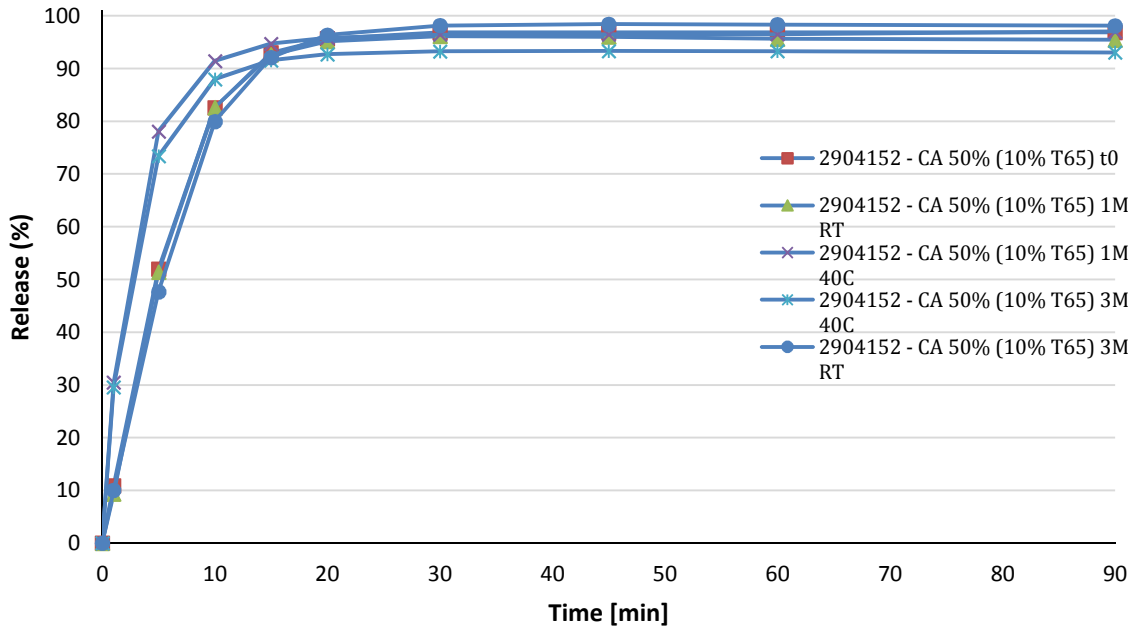

Figure 27. Dissolution profile of Ibuprofen microcapsules containing 50% coating and 10% Tween® 65

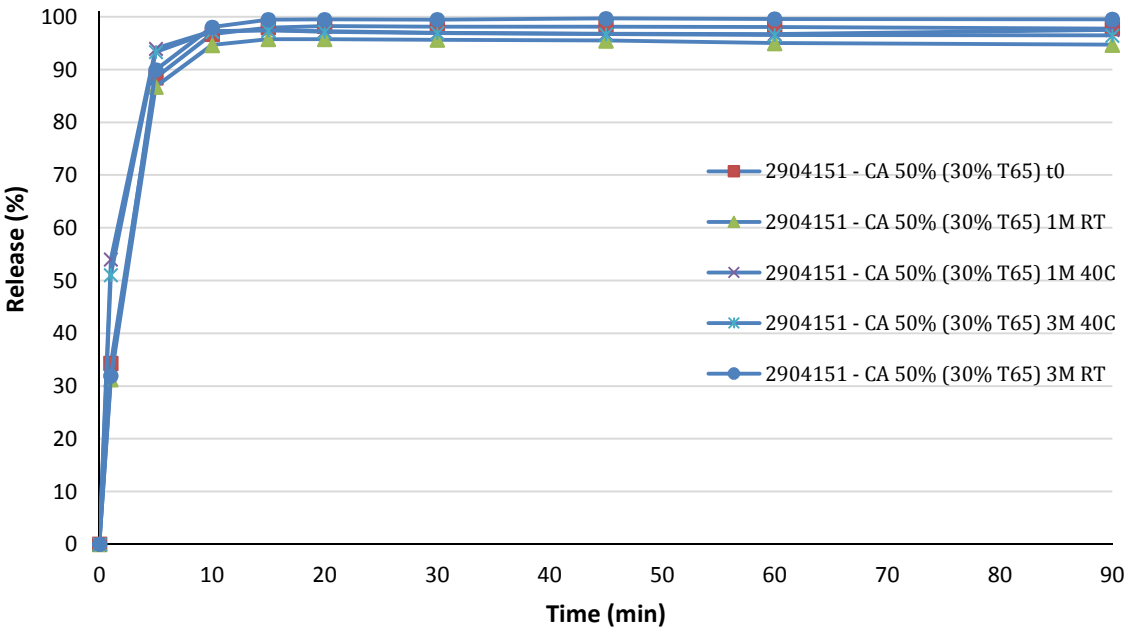

Figure 28. Dissolution profile of Ibuprofen loaded microcapsules containing 50% coating and 30% Tween® 65

Figures 29 and 30 present the release profile of the samples with 70% coating amount containing 10% and 30% of Tween® 65 in the coating.

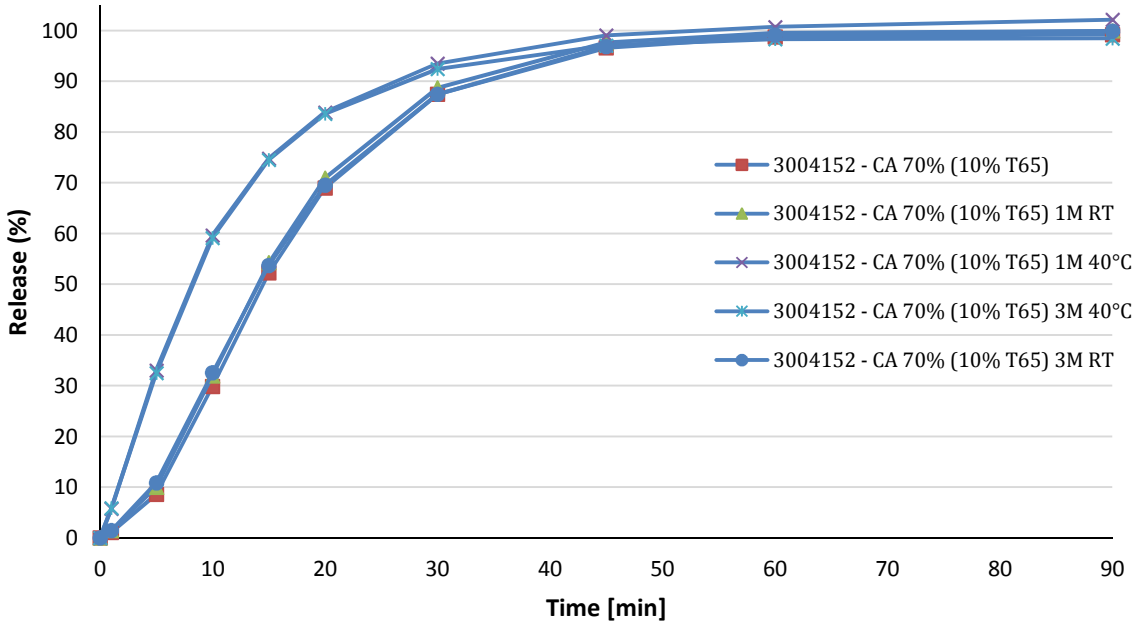

Figure 29. Dissolution profile of Ibuprofen loaded microcapsules containing 70% coating and 10% Tween® 65.

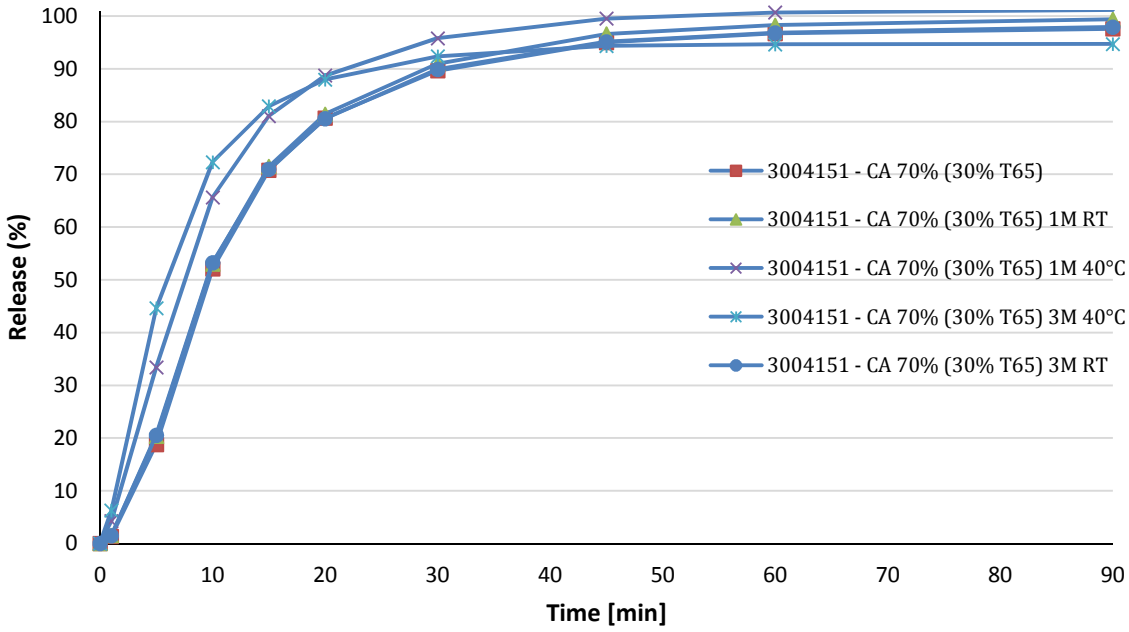

Figure 30. Dissolution profile of Ibuprofen loaded microcapsules containing 70% coating and 30% Tween® 65

Although generally fast, the release profile of the Ibuprofen sodium dihydrate containing microcapsules with 70% of coating amount is significantly slower than the profile of the samples with 50% of coating. The effect of the storage depending on the amount of emulsifier can be observed and compared with the profiles of the NAc microcapsules.

More specifically, both microcapsules with 50% and 70% coating amount but 10% emulsifier (Figures 27,29) show a significantly accelerated release after storage in 40°C for one month (f2=47 and f2=40 respectively). On the contrary after storage in room temperature for one month the differences are insignificant (f2=93 and f2=89 respectively).

The dissolution profiles of the formulation after 3 months of storage remain also in that case almost identical compared with the ones after 1 month (f2=73 for 40°C storage, f2=80 for room temperature for the 50% coated sample and f2=86 for 40°C storage, f2=95 for room temperature for the 70% coated sample).

Taking a look at the dissolution profiles of the formulations with 30% emulsifier content, the same tendency as with NAc is observed.

The microcapsules with 50% coating amount and 30% emulsifier show insignificant changes on the dissolution profile after storage in both conditions and for both time spans, with a f2 varying from 58 to 92.

The microcapsules with 70% coating amount and 30% emulsifier show also insignificant changes with the exception of the direct comparison between the most extreme conditions (time zero and three months in 40°C) where the f2 value is 46. All other values vary between 53 and 95, indicating insignificant difference between the release profiles.

It is important to mention in that point that the hot-melt coating procedure of the formulations containing 30% Tween® 65 were the most problematic, considering the nature of the emulsifier -highly viscous/sticky at process temperatures between 25 and 30°C leading to accumulation of material on the walls of the fluid bed product container. Especially having 70% coating amount increased highly the process time thus the particle loss in the filters due to the friability. In the case of Ibuprofen sodium dihydrate granules, this phenomenon was even more pronounced, because granules have per se higher friability than API crystals like NAc.

5.1.3 Citric acid

As with the previous APIs, the following figures (Figures 31-34) present the release profiles of the microcapsules containing citric acid.

Figures 31 and 32 show the release of the samples with 50% of coating amount (10% and 30% of Tween® 65 in the coating).

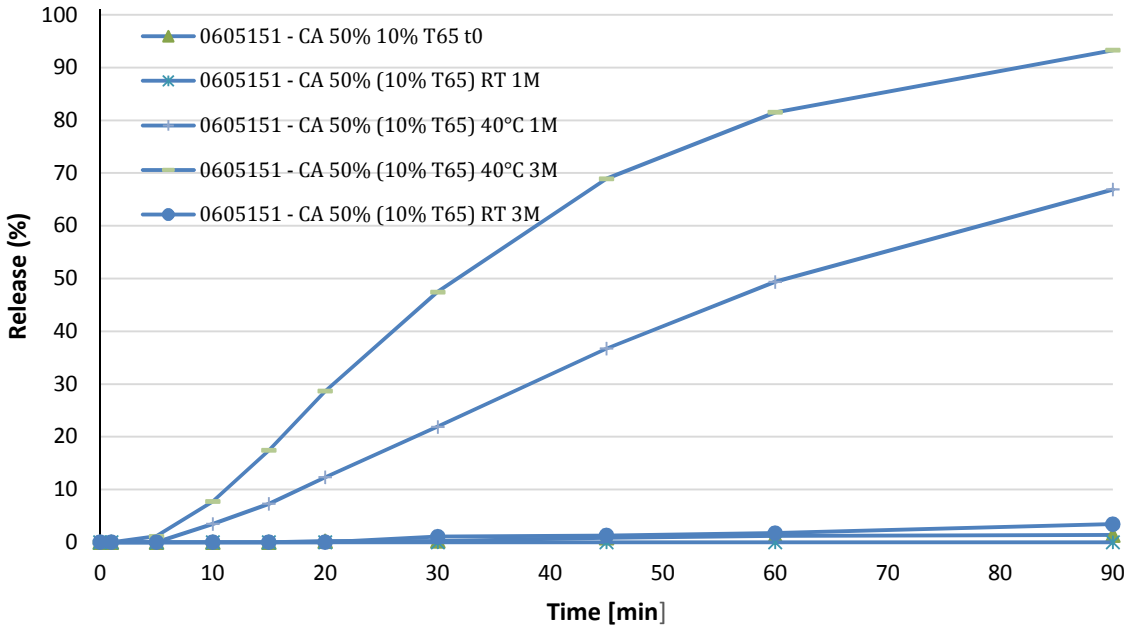

Figure 31. Dissolution profile of citric acid microcapsules containing 50% coating and 10% Tween® 65

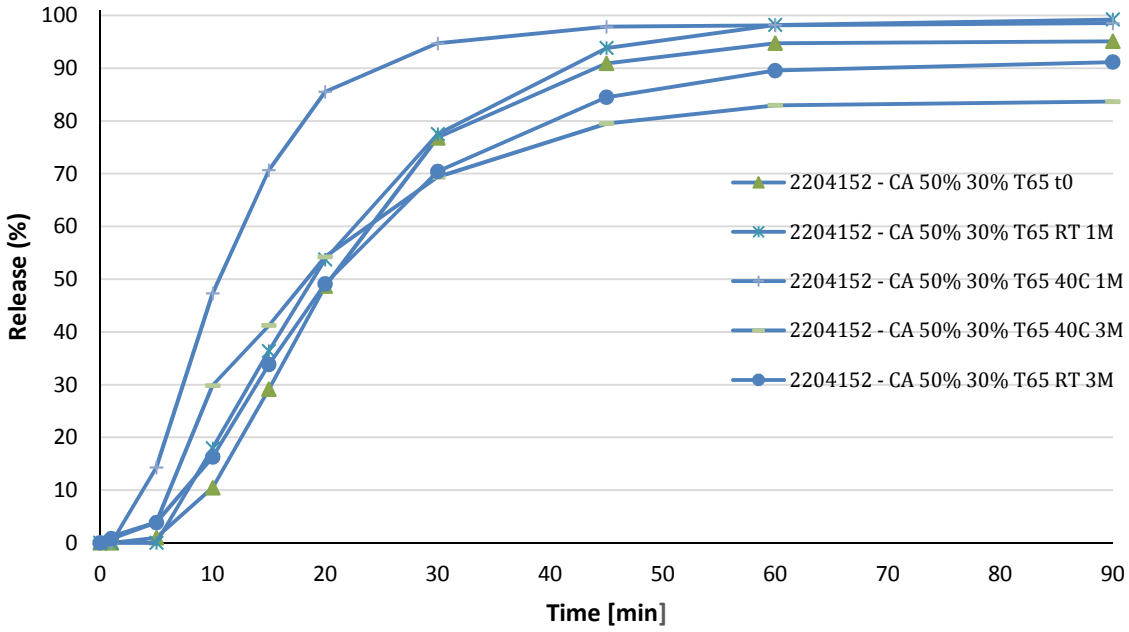

Figure 32. Dissolution profile of citric acid microcapsules containing 50% coating and 30% Tween® 65

Figures 33 and 34 present the release profile of the samples with 70% coating amount containing 10% and 30% of Tween® 65 in the coating.

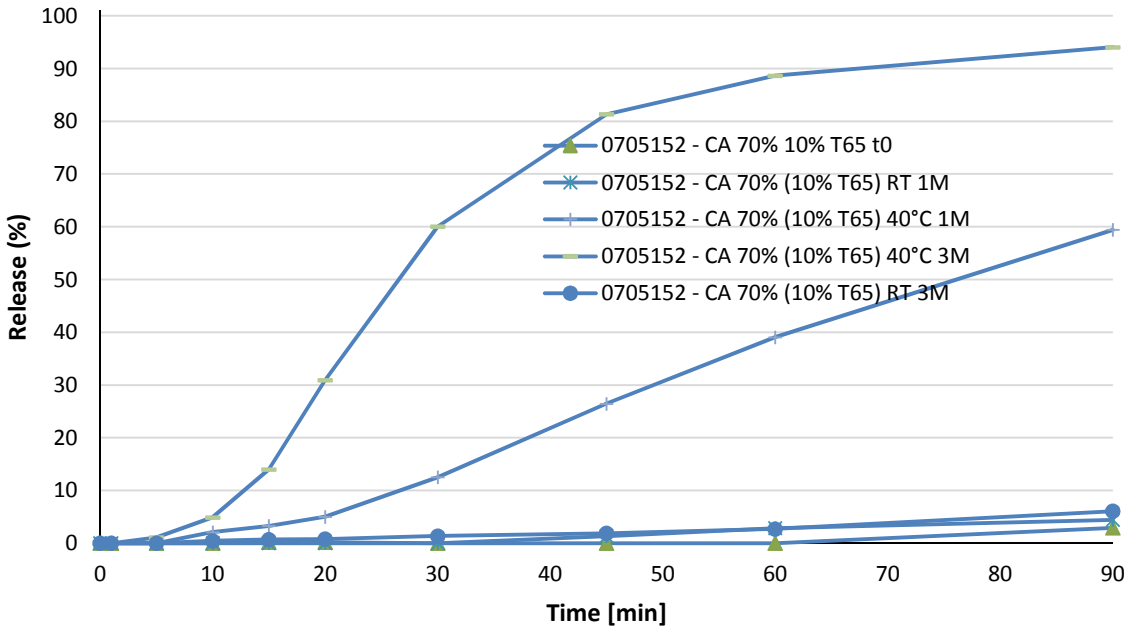

Figure 33. Dissolution profile of citric acid microcapsules containing 70% coating and 10% Tween® 65

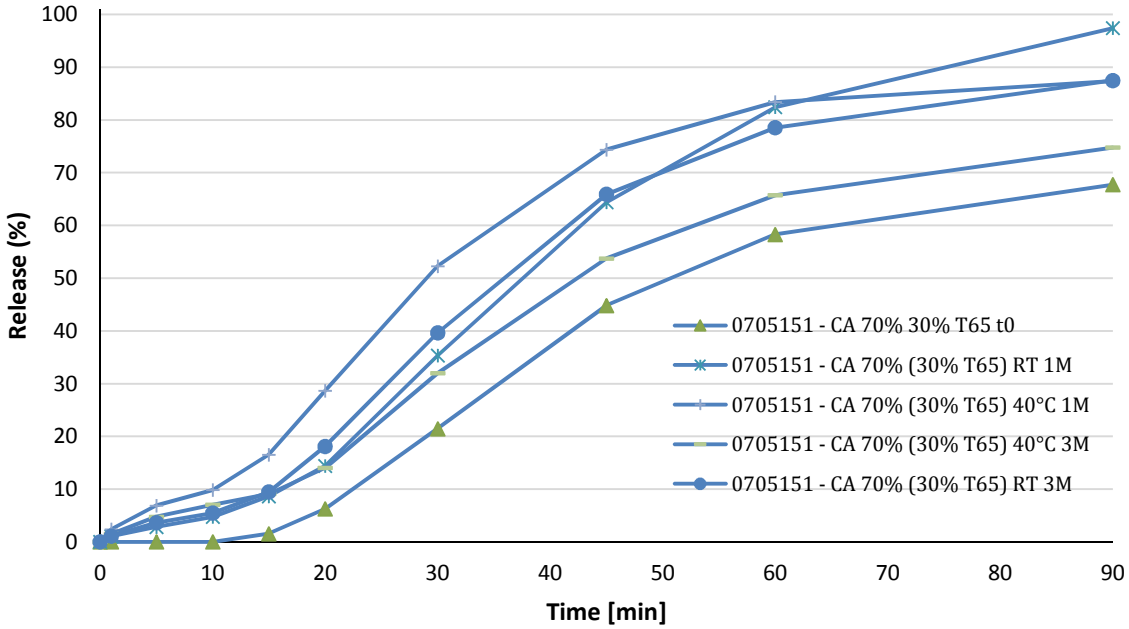

Figure 34. Dissolution profile of citric acid microcapsules containing 70% coating and 30% Tween® 65

The release profile of the citric acid containing microcapsules with 70% of coating amount is significantly slower than the profile of the samples with 50% of coating.

It can be also easily observed, that the amount of Tween® 65 in the coating strongly influences the profile towards much quicker release.

Microcapsules with 50% and 70% coating amount and 10% emulsifier (Figures 31, 33) show a significantly accelerated release after storage in 40°C for one month (f2=26 and f2=30 respectively), which is much markedly compared to the release profile of NAc and Ibuprofen sodium dihydrate. On the contrary, after storage in room temperature for one month the differences are insignificant (f2=96 and f2=91 respectively).

Some differences between the release profiles of citric acid and the previous APIs can be however pointed out. The first difference is that the dissolution profiles of the formulation after 3 months of storage in 40°C do not remain identical compared with the ones after 1 month (f2=34 for 40°C storage for the 50% coated sample and f2=24 for 40°C storage for the 70% coated sample).

On the other hand, the profile remains almost identical after storage in room temperature (f2=88 for room temperature for the 50% coated sample and f2=94 for room temperature for the 70% coated sample).

Taking a look at the dissolution profiles of the formulations with 30% emulsifier content, the second difference can be observed. While storage for one month at 40°C did increase the release rate as expected (f2=31 with 50% coating amount and f2=35 with 70% coating amount), three months storage at 40°C showed a decrease of that rate, reaching f2 values that are either close or in the margin of being characterized as identical with the release rate of the time zero measurements (f2=49 with 50% coating and f2=56 with 70% coating amount).

As mentioned in the case of Ibuprofen granules, the production of microcapsules containing 70% coating and 30% emulsifier is the most problematic leading to particles with uneven coating distribution. Although the citric acid crystals are less friable than the Ibuprofen granules, the high amount of Tween® 65, given the viscous-sticky nature of the emulsifier, as well as the high amounts of coating, which drastically increases the process time, seems to still negatively influence the process.

5.2 Differential Scanning Calorimetry

5.2.1 Tripalmitin and Tween® 65 blends

5.2.1.1 Thermograms

In the following figures (Figures 35-41) the thermograms of pure tripalmitin as well as with increasing amount of Tween® 65 can be observed. Figure 41 shows the thermogram of pure Tween®65 in the same storing conditions.

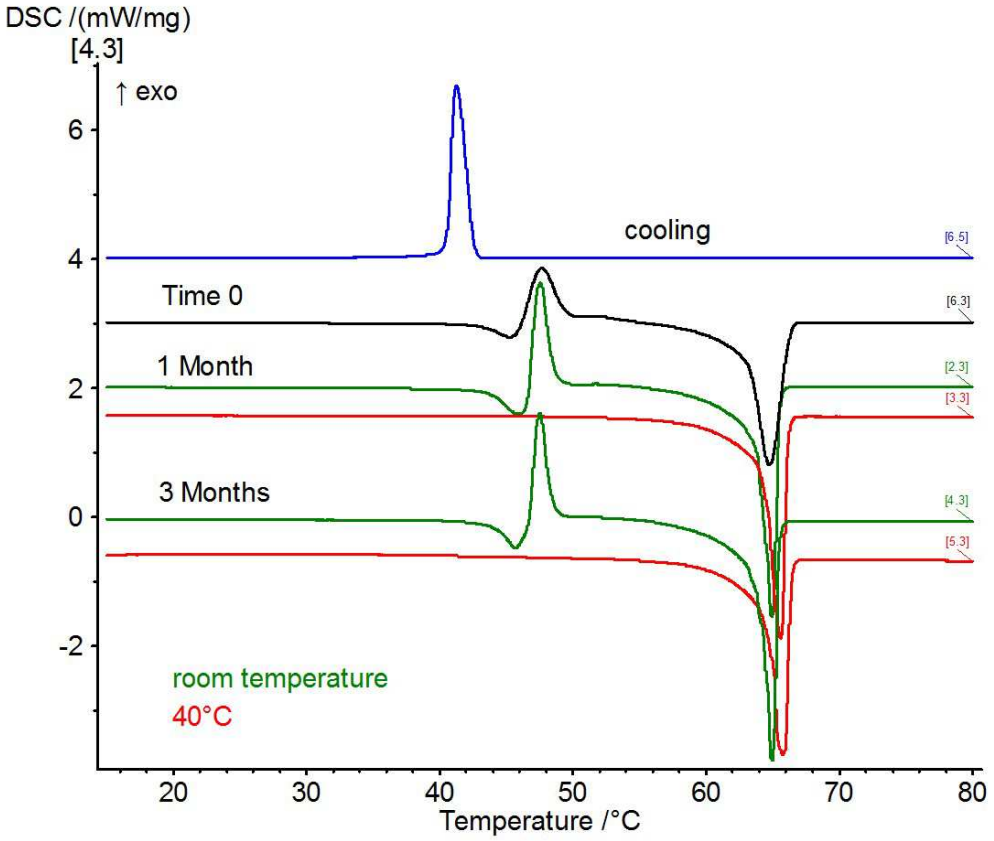

Figure 27. Thermograms of pure tripalmitin

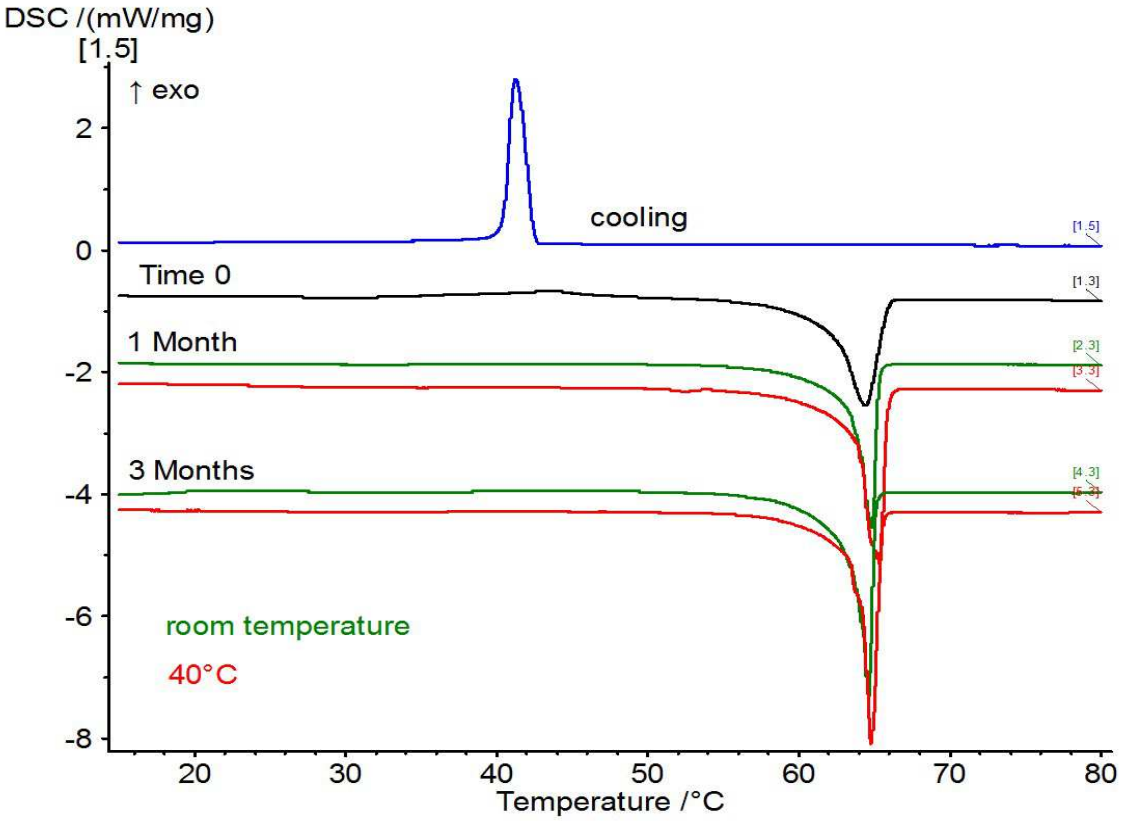

Figure 28. Thermograms of tripalmitin with 10% Tween® 65

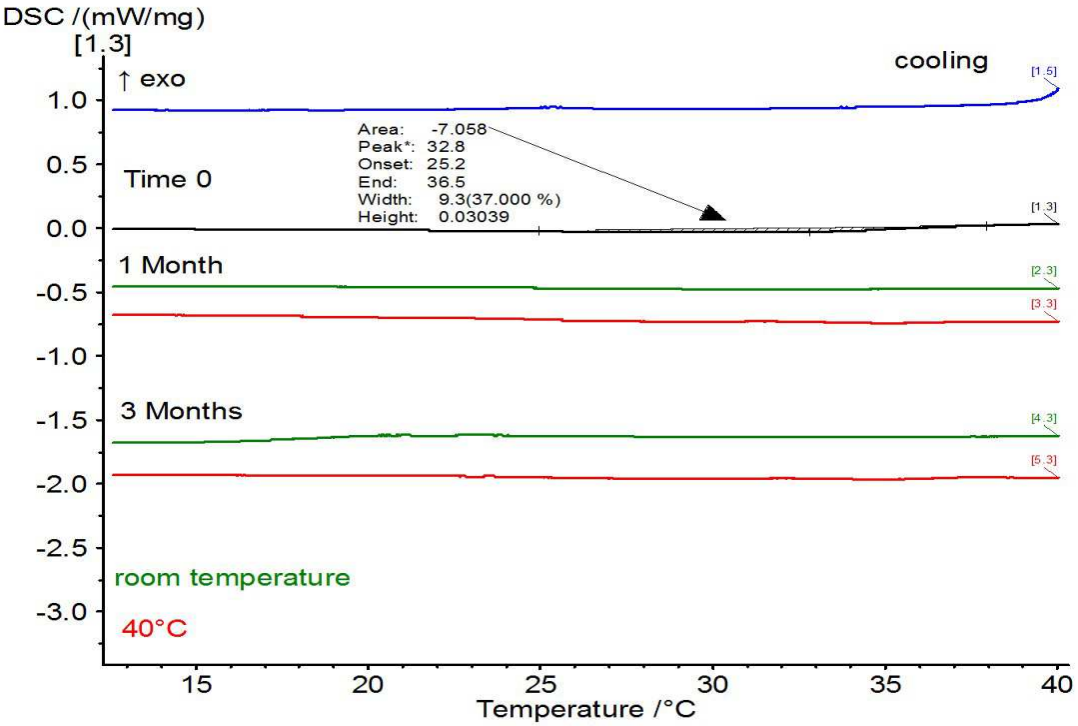

Figure 29. Zoom into the endothermic peak of Tween® 65 present in the previous mixture

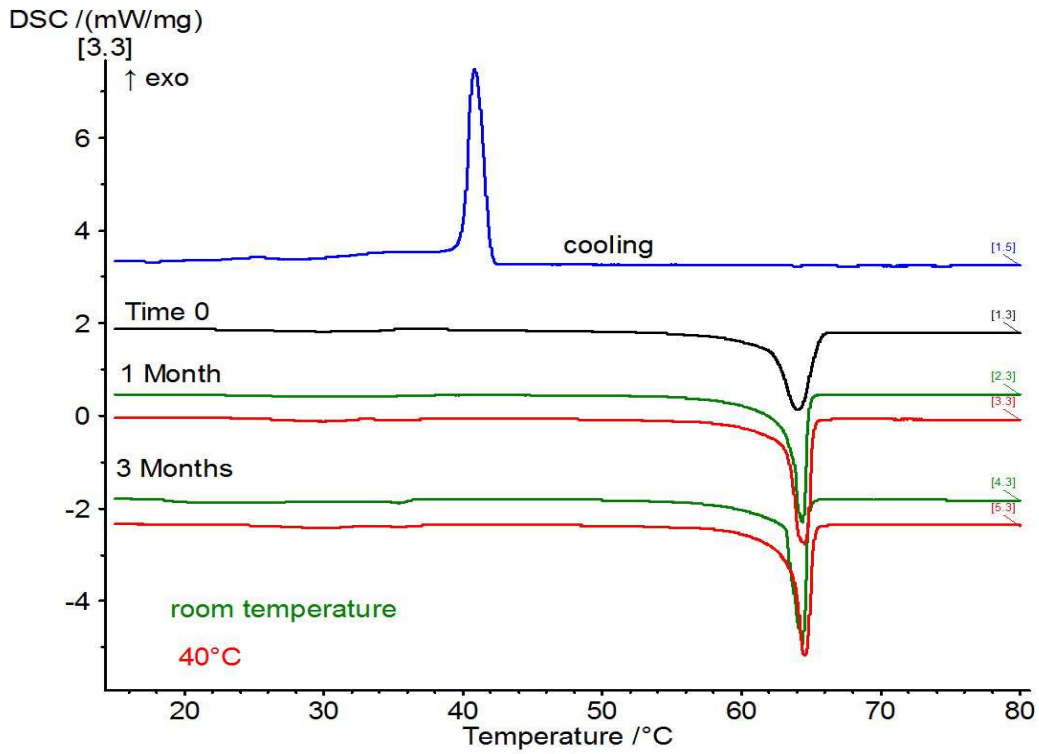

Figure 30. Thermograms of tripalmitin with 25% Tween® 65

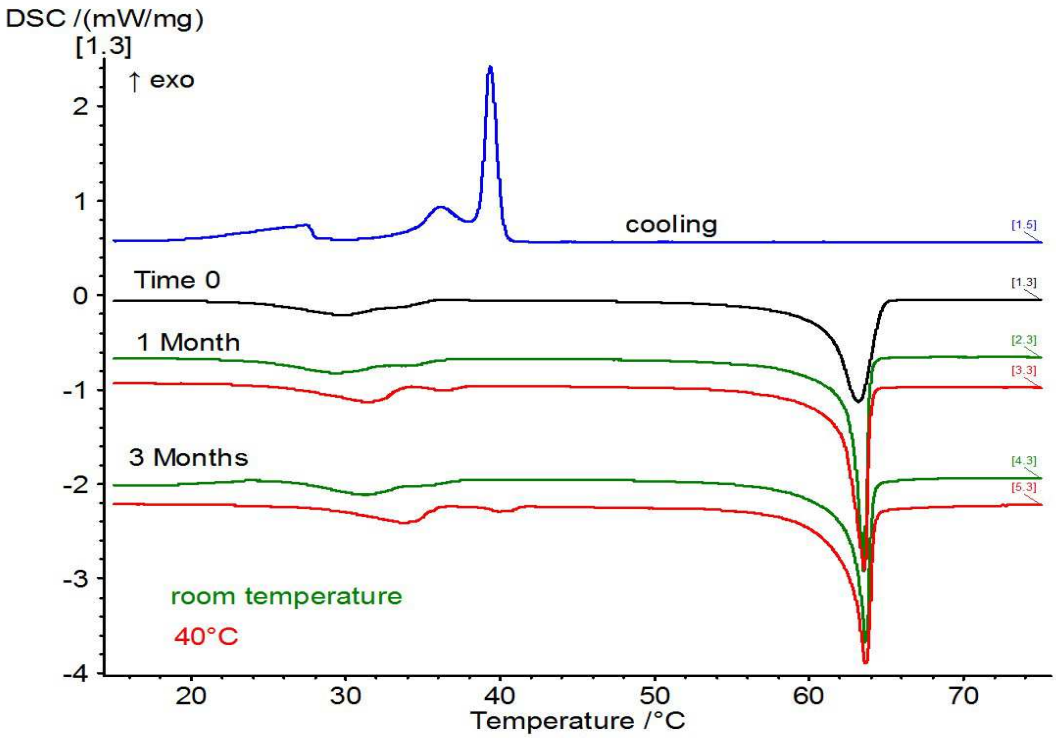

Figure 31. Thermograms of tripalmitin with 50% Tween® 65

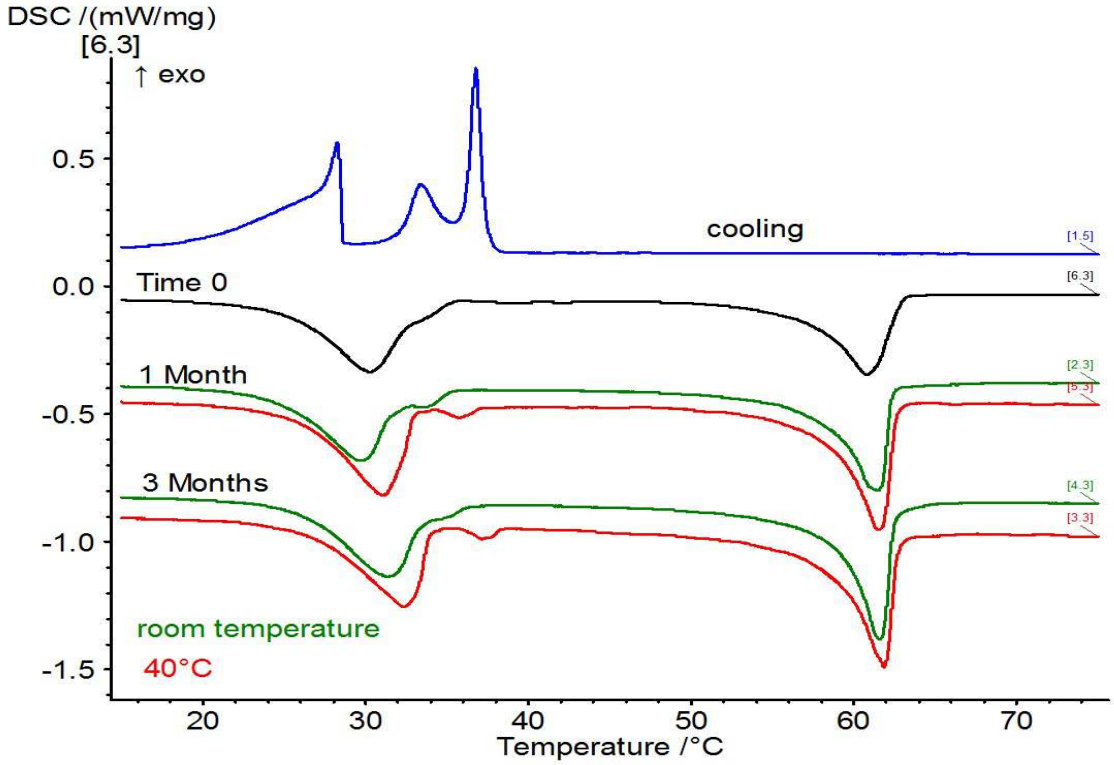

Figure 32. Thermograms of tripalmitin with 75% Tween® 65

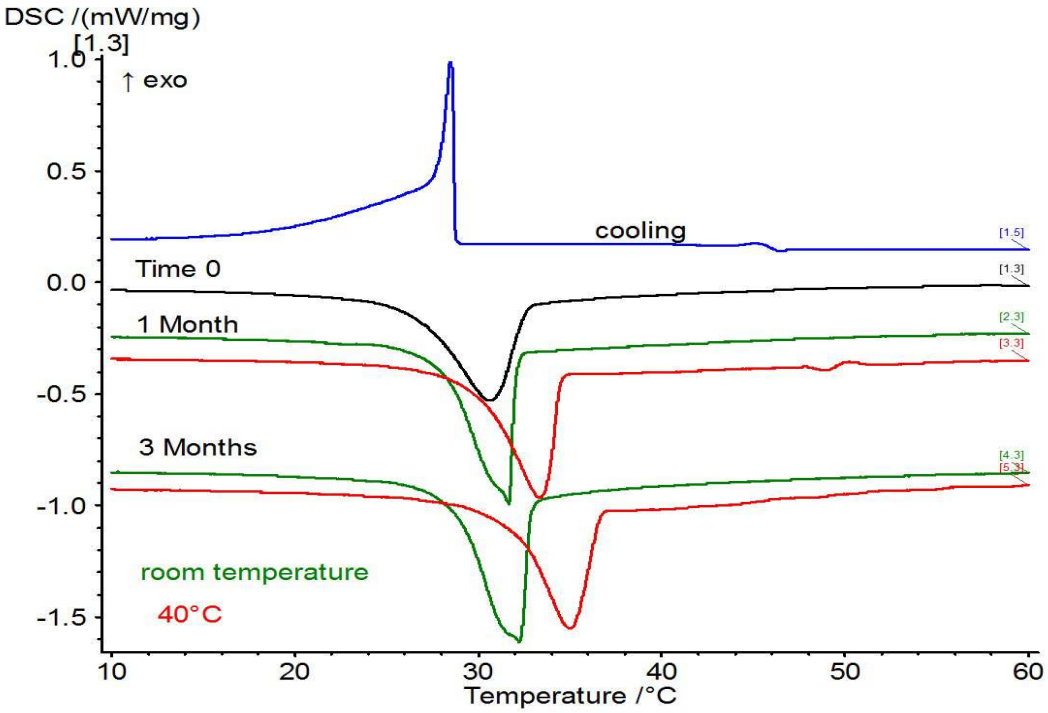

Figure 33. Thermograms of pure Tween® 65

Analyzing the thermodynamic behavior of pure tripalmitin with DSC we observe the melting endothermic peak of the α form at 45°C followed by the crystallization of β and finally the melting of the β form at about 65°C. The intermediate forms β'_1 and β'_2 are not observed in the broad exothermic peak of crystallization as for this to happen the temperature has to be hold steady for a specific amount of time only slightly above the melting point of the α-form [7].

The effect of temperature on the crystallization and the thermal profile of Tripalmitin is clear: while storing in room temperature for one and three months do not change the DSC profile (apart from the sharpening appear of the melting and crystallization peaks), storing the samples at 40°C significantly changes the profile. Already after the first month the total amount of the sample has been tranformed into the β-form and only the endothermic melting peak of which appears on the thermogram.

Adding 10% of Tween® 65 in the mixture causes a much quicker transformation of the lipid to the β-form even in room temperature after one month. Even at time 0, most of the tripalmitin is already in the β-form, however some α-form still exists the enthalpy of which can be observed on the phase diagrams that follow. A melting peak of Tween® 65 is also present however it is quite small and only visible after zooming into the temperature area between 25-40°C (Fig. 36).

As the percentage of Tween® 65 increases in the mixtures, the α-form completely disappears already since time 0. Not only that, but a second peak appears during the heating and cooling of the samples. This peak is shifted towards higher temperatures after storage of the samples at 40°C. The temperature range where this peak appears (<40°C) and the conditions under which it is more expressed (stored at 40°C and by increasing Tween® 65 amount in the mixture) are indications showing that this peak is not caused by any remaining α-form of the lipid. A possible explanation could be the forming of a co-crystal between the lipid and emulsifier. Storing the samples at 40°C ensures the presence of Tween® 65 in liquid form. Having higher mobility the emulsifier molecules-which also prevail in the mixture as this phenomenon is easier observed when having at least 50% of the emulsifier in the mixture-can be merged into the lipid molecules forming a type of co-crystals. However, further research has to be made in this direction.

This second peak is easier to observe during the cooling of the samples. The same heating/cooling program (2K/min) was applied to samples containing tristearin and Tween® 65 and the result was that this peak, although smaller, was still present. This proves the fact that it is not dependent on the length of the alkyl chain of the lipid but it appears during the coexistence of a TAG and high amounts of Tween® 65 in the mixture.

In the last thermogram (Fig. 41) the melting behavior of pure Tween® 65 can be observed. No differences are obvious apart from the fact that with aging in elevated temperature conditions, the melting peak appears to be shifted towards higher temperatures. Similar to the behavior of lipids, raising the temperature only some few degrees over the melting point (Tween® 65 melting point: 31-35°C) does not erase all the crystal memory. Tween® 65 has a broad melting endotherm due to its heterogeneity in terms of PEG-ylation and esterification of the sorbitan molecule. For this reason, a possible explanation could be a parallelism with the 'melt-mediated transformation' where more stable forms recrystallize after the melting of less stable forms [7]. Another theory, could be the fact that with the temperature just above the melting point, the crystal structures of Tween® 65 that have not already molten could grow in size due to the increased mobility.

5.2.1.2 Phase diagrams

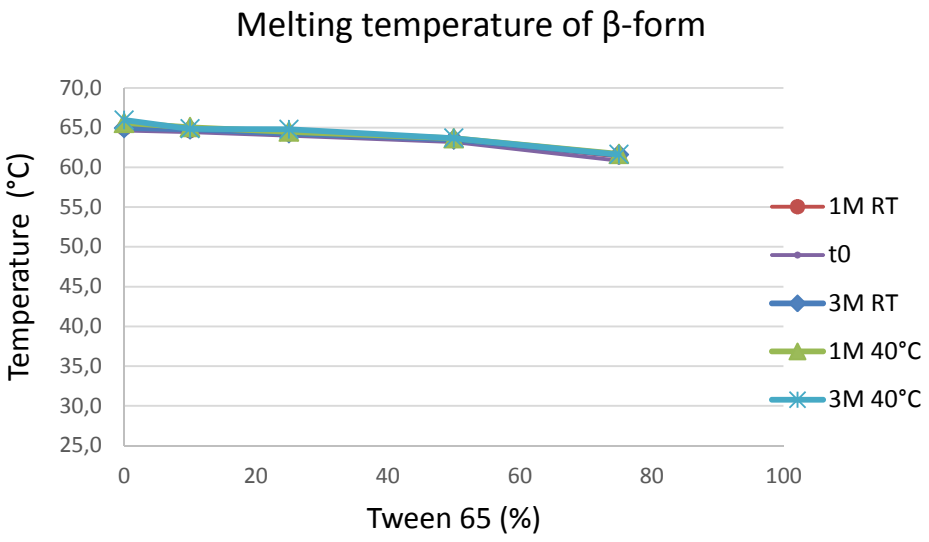

Figure 34. The melting point of Tripalmitin as a function of the Tween® 65 percentage

The first figure shows how the increasing amount of Tween® 65 slightly influences the melting temperature of the β-form of tripalmitin. Tween® 65 behaves as an impurity thus the lowering of the melting point of tripalmitin is an expected behavior as the crystal lattice of tripalmitin is disrupted[33]. Temperature and length of storage do not seem to influence the results.

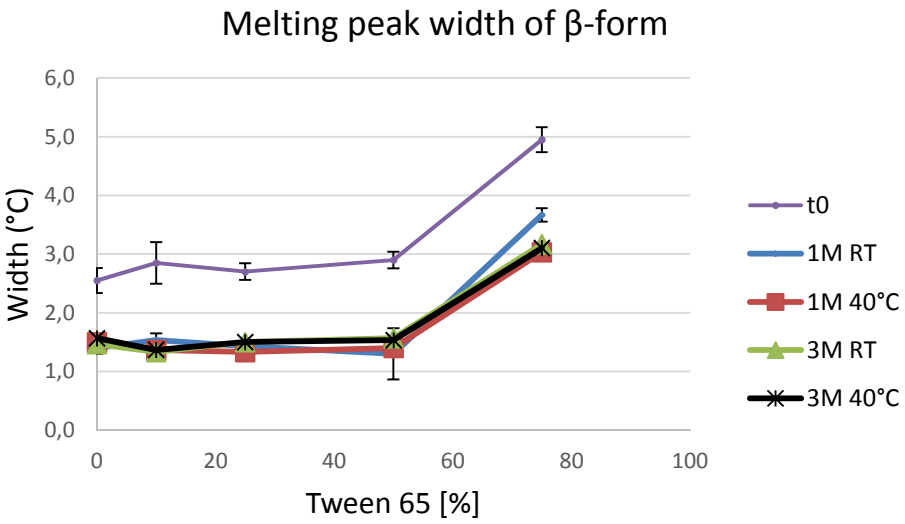

Figure 35. Melting peak width of tripalmitin as a function of the Tween® 65 percentage

In the second diagram (Figure 43), the peak width of the melting peak of the β-form shows an interesting behavior. With up to 50% of Tween® 65, it remains stable and only with 75% of Tween® 65 the peak width increases drastically. This could indicate that the addition of Tween® 65, even at high concentrations, does not have any impact on the melting peak width of the β-form of tripalmitin.

It is also interesting to look at the effect of aging; the peak width is significantly lowered after storage of the samples and the sharper peaks could indicate a tighter packing of the crystal lattices of the lipid. This difference is also statistically significant ($p<0,05$). One can also observe that the conditions and length of the storage showed no significant impact on the peak width.

These two points could be in contrary with what was previously observed when the dissolution profiles where analyzed and indicated faster release of the samples stored at

40°C. It seems thus that the peak width ie. the packing of the crystals, although tighter, was not the reason for instable dissolution profile after storage, as the presence of the emulsifier dominated and controlled the behavior, providing a faster dissolution profile.

5.2.2 Dynasan 118 and Tween 65 blends

5.2.2.1 Thermograms

In the following figures (44-48) the thermograms of pure tristearin as well as with increasing amount of Tween® 65 can be observed.

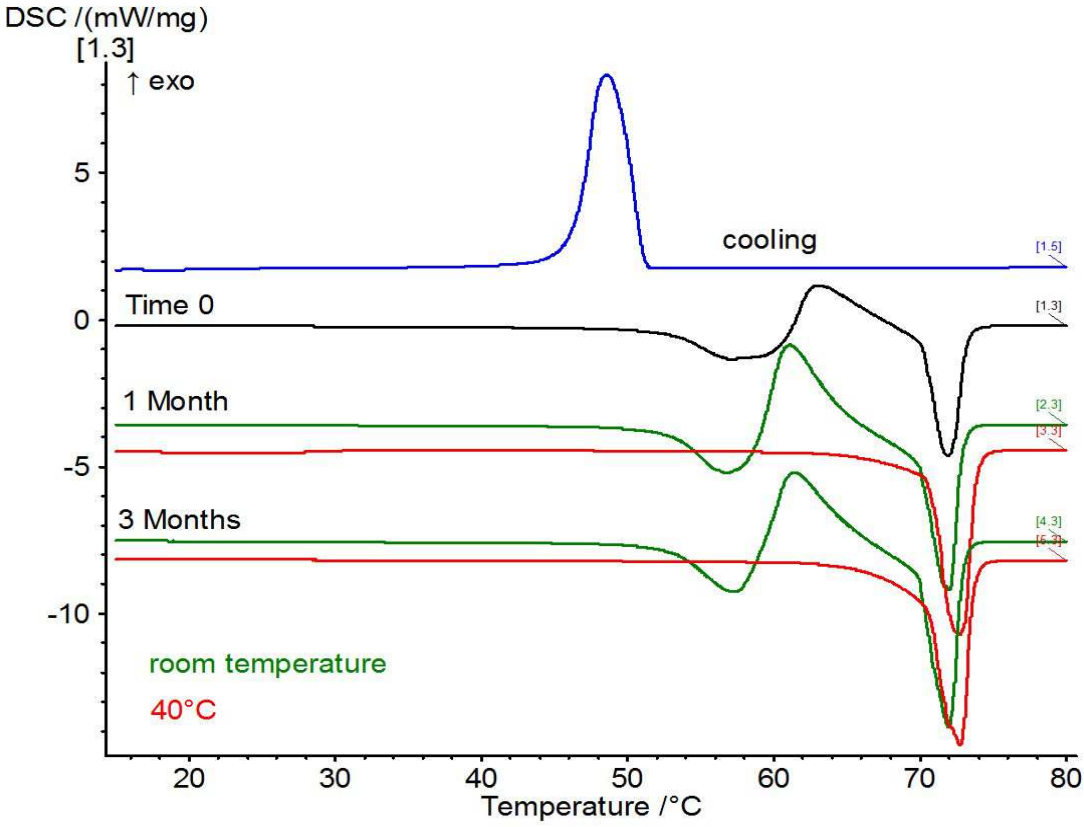

Figure 36. Thermograms of pure tristearin

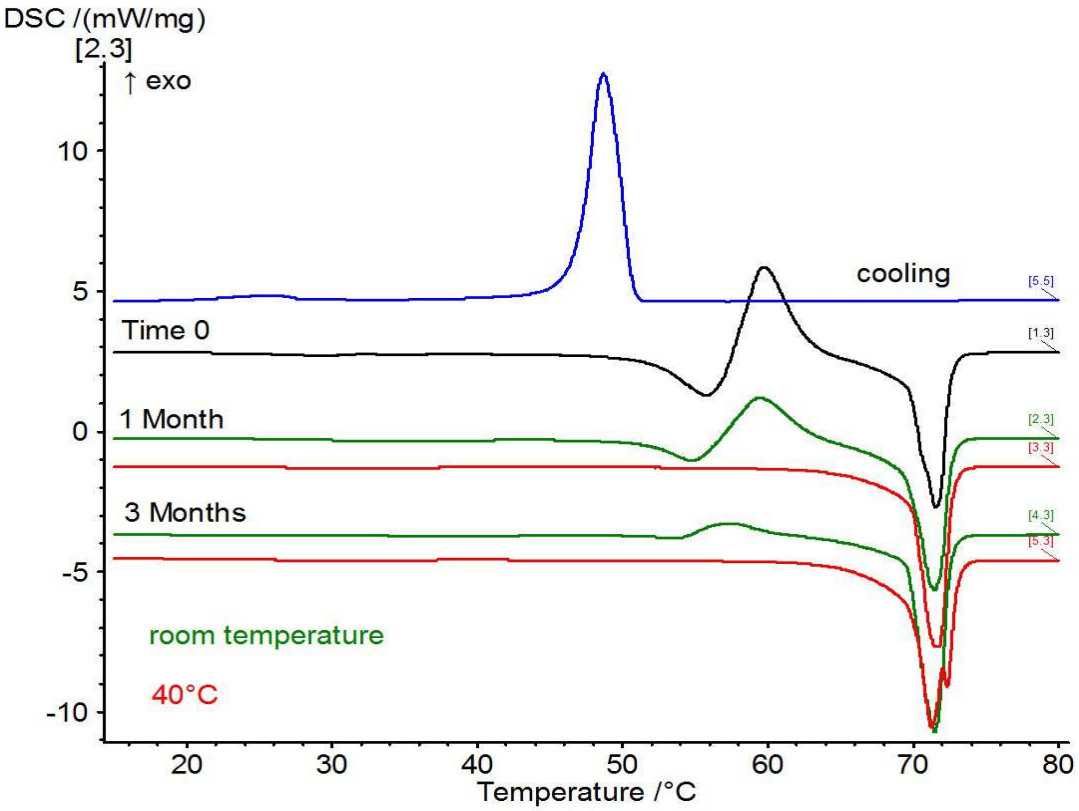

Figure 37. Thermograms of tristearin with 10% Tween® 65

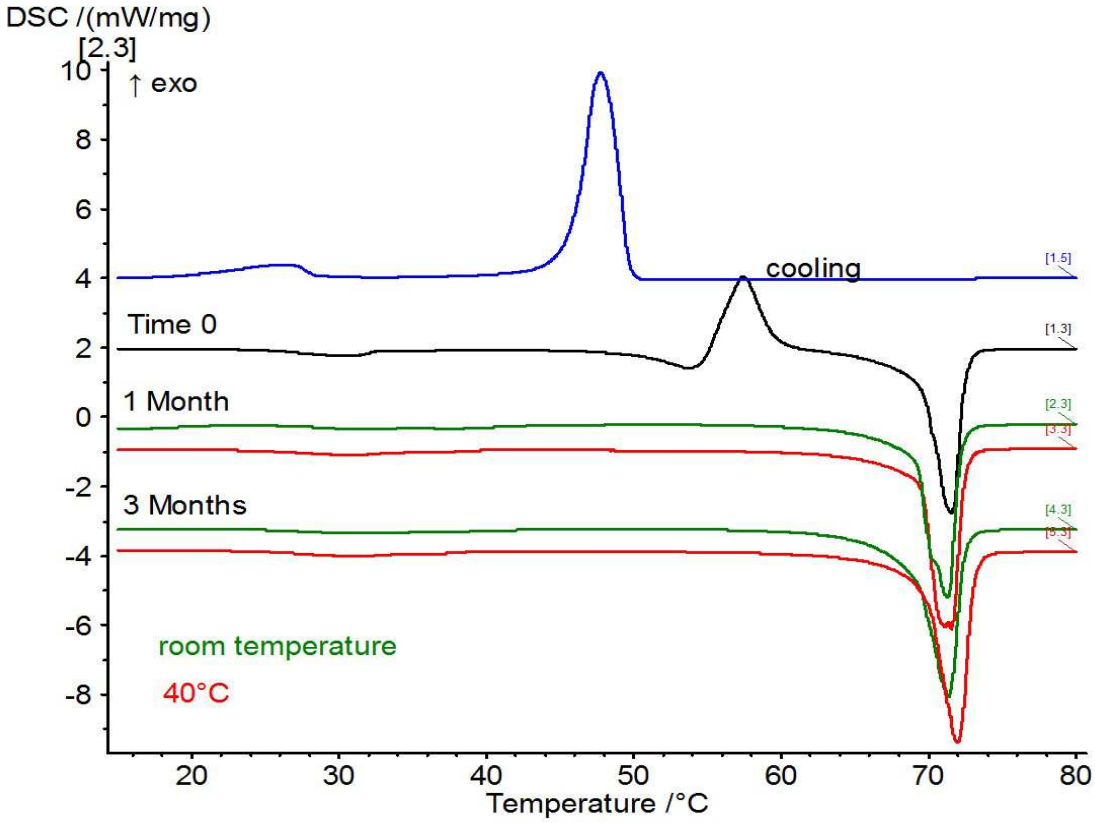

Figure 38. Thermograms of tristearin with 25% Tween® 65

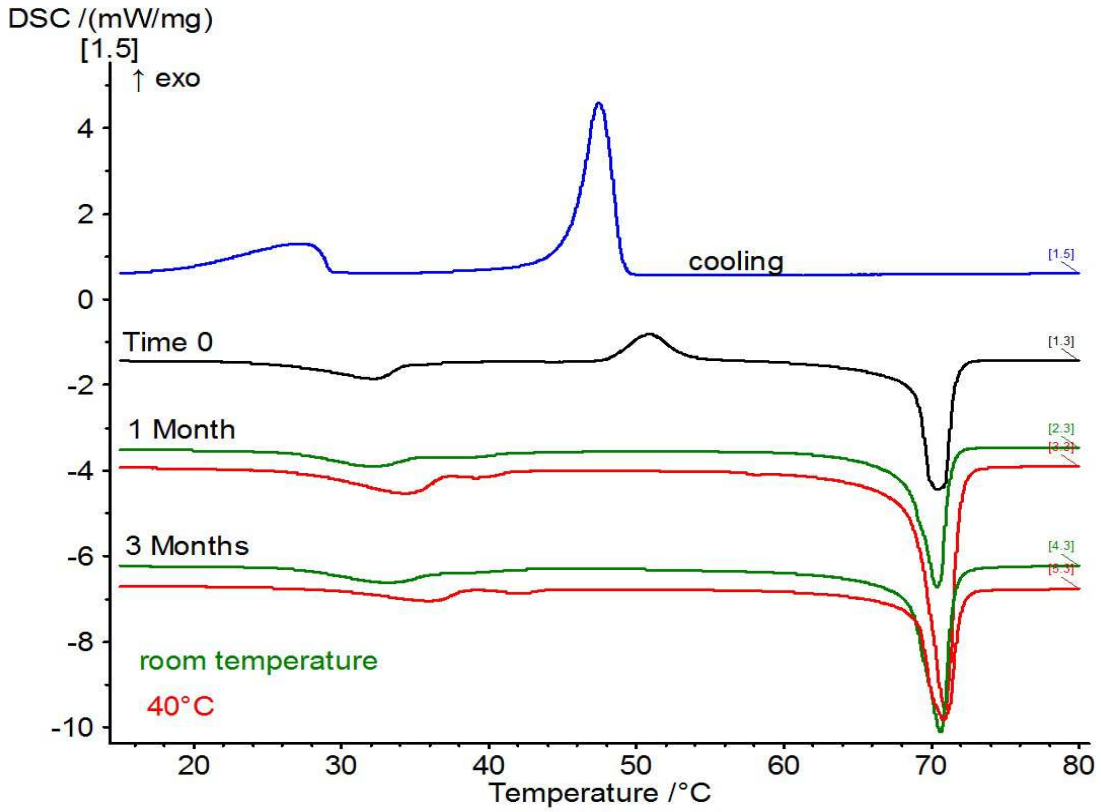

Figure 39. Thermograms of tristearin with 50% Tween® 65

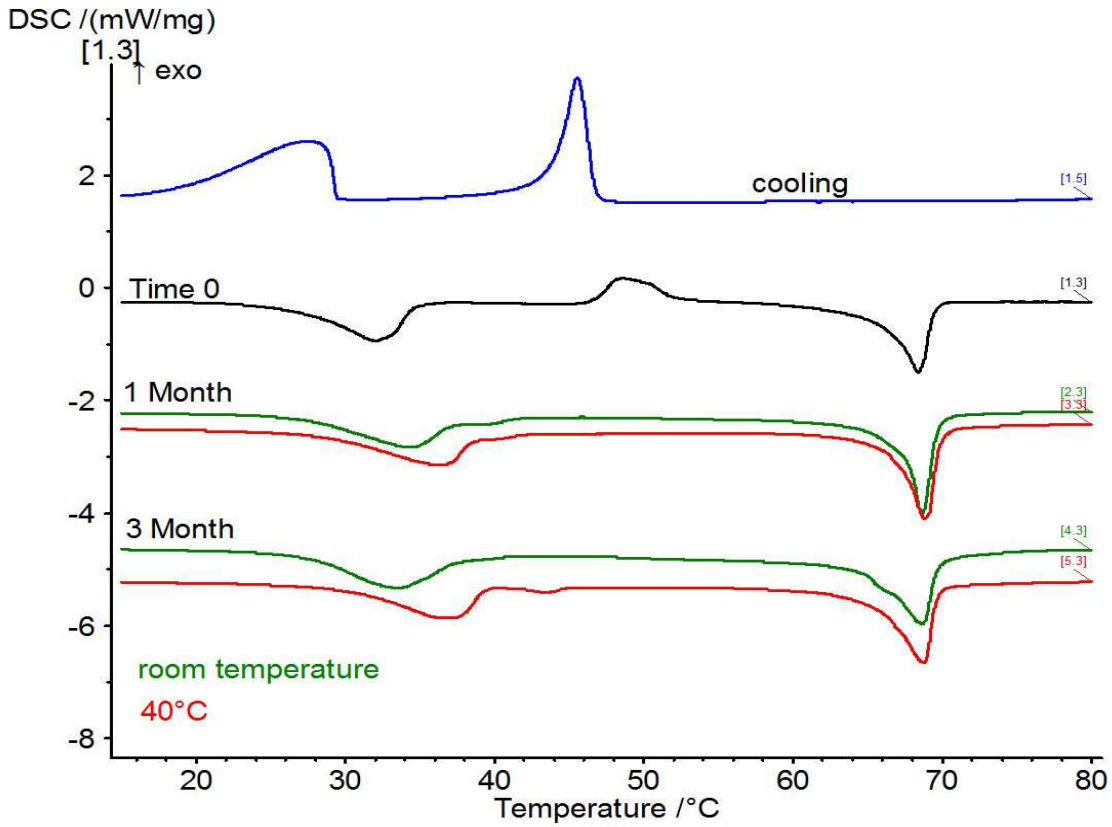

Figure 40. Thermograms of tristearin with 75% Tween® 65

Analyzing the thermograms of tristearin we observe a comparable behavior as with that of Tripalmitin. Pure Tristearin shows the melting endothermic peak of the α-form at about 57°C followed by the crystallization of β and finally the melting of the β form at 72°C.
The intermediate forms β'_1 and β'_2 are also in that case not observed.
Storage under elevated temperature causes again changes on the crystallization and the thermal profile of tristearin: stored in room temperature, the samples of pure tristearin are stable while stored at 40°C causes the quick transformation of the the α-form to the β-form as a whole already after the first month.
Adding 10% of Tween® 65 in the mixture causes a quicker transformation to the β-form in room temperature: after three months the α-form is barely visible. While the melting peak of Tween® 65 is not clearly visible, we can observe the crystallization peak of Tween® 65 during the cooling in the temperature area 22-30°C.

By increasing percentage of Tween® 65 in the mixtures, the α-form does not completely disappear during the time 0 measurements. In all mixtures an exothermic peak indicating the crystallization of the β-form is visible which means that there is still some amount of tristearin in the α-form. This is a difference compared to tripalmitin and it has been observed in previous works where, in the presence of Tween® 65, the enthalpy of the α-form of tripalmitin was much more decreased than in the case of tristearin [34].
Another effect observed in the presence of high amounts of Tween® 65 is the shifting of the crystallization peak of the β-form towards lower temperatures.

As mentioned before, the melting peak of Tween® 65 is visible even at low concentrations in both mixtures with tripalmitin and tristearin. This indicates that the lipid and the emulsifier do not form one phase when they are mixed in the concentration tested in this work.

5.2.2.2 Phase diagrams

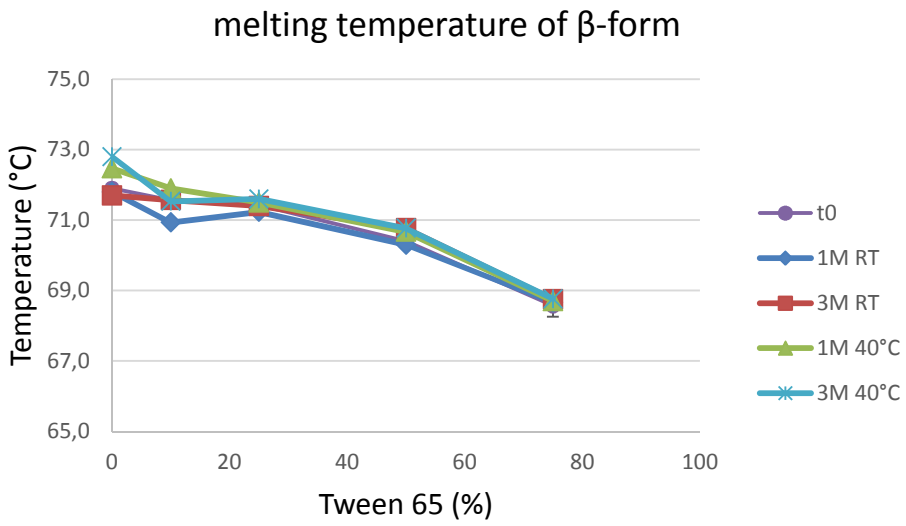

Figure 41. Melting temperature of tristearin as a function of Tween® 65 concentration

The behavior of the melting temperature of tristearin in presence of Tween® 65 seems similar to that of tripalmitin. Increasing amounts of Tween® 65 slightly suppress the melting point of tristearin and the temperature and length of storage do not influence the results as well.

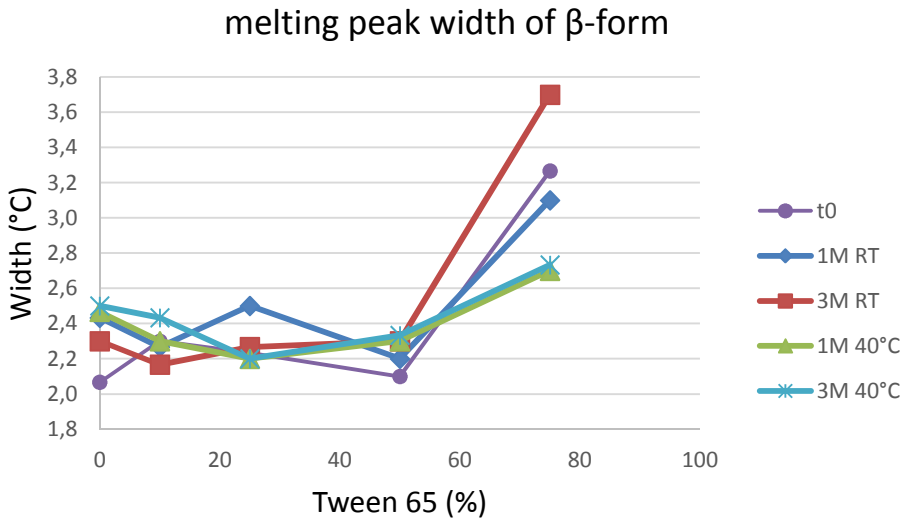

Figure 42. Melting peak width of tristearin as a function of Tween® 65 concentration

The tendency of peak broadening by increasing amount of Tween® 65 is also in the case of tristearin present. However, in contrary to the mixtures of tripalmitin, storage does not seem to play a role in the peak width. This might be explained by the higher arrangement of the crystalline structures of tristearin compared to tripalmitin.

In contary to various previous studies [35] where sorbitan tristearate (Span 65) with high lipophilicity (HLB=2,1) was used as an emulsifier in mixtures with TAGs, Tween® 65 has an HLB of 10,5 which categorizes it to the slightly lipophilic emulsifiers. Thus the solubility of Tween® 65 in the molten lipid is much lower. Also having a melting point under 40°C, Tween® 65 does not form an eutectic mixture with any of the lipids used.

It can be assumed that the immiscible lipids and Tween® 65 form a type of dispersion; when in molten state, the dispersion consists of a liquid lipid and a liquid O/W emulsifier. When in solid state, the crystallized materials form a solid-solid dispersion. During storage in room temperature, the dispersion remains generally stable. However, when stored in 40°C, one of the components-in this case the emulsifier-is in molten state which results in a (partial) separation of the two components.

5.3 Particle Size Distribution

The particle size distribution of all samples after production as well as of all the pure APIs was calculated and presented in the table 12.

Sample	X_{50} (µm)	X_{10} (µm)	X_{90} (µm)	X_{90}/X_{10}	SPAN*	Aspect ratio (a_{50})
Citric acid pure	796,74 +/- 22,63	520,23 +/- 15,05	1113,38 +/- 11,23	2,14	0,744	0,7651
Citric acid 50% CA (10% T65)	929,44 +/- 105,96	686,84 +/- 55,39	1213,54 +/- 137,26	1,76	0,567	0,8195
Citric acid 50% CA (30% T65)	961,01 +/- 22,06	709,92 +/- 10,92	1296,48 +/- 27,16	1,83	0,610	0,8247
Citric acid 70% CA (10% T65)	1119,30 +/- 88,53	819,35 +/- 52,10	1480,97 +/- 182,10	1,8	0,591	0,8408
Citric acid 70% CA (30% T65)	1288,16 +/- 14,69	1006,65 +/- 2,62	1662,47 +/- 12,02	1,65	0,509	0,8623
NAC pure	527,31 +/- 0,48	437,02 +/- 2,14	651,91 +/- 2,51	1,49	0,408	0,6591
NAC 50% CA (10% T65)	619,92 +/- 2,76	480,86 +/- 3,39	776,28 +/- 2,15	1,61	0,477	0,7452
NAC 50% CA (30% T65)	724,62 +/- 6,54	574,84 +/- 2,62	951,90 +/- 16,29	1,66	0,520	0,7339
NAC 70% CA (10% T65)	789,70 +/- 5,44	676,97 +/- 2,74	962,76 +/- 0,29	1,42	0,362	0,7598
NAC 70% CA (30% T65)	941,37 +/- 16,75	710,76 +/- 24,18	1292,96 +/- 33,37	1,82	0,618	0,7606
Ibuprofen-Na granules	376,22 +/- 7,82	158,22 +/- 1,52	664,15 +/- 3,09	4,2	1,345	0,6475
Ibuprofen-Na 50% CA (10% T65)	431,93 +/- 12,71	241,31 +/- 7,03	758,70 +/- 8,59	3,15	1,198	0,7332
Ibuprofen-Na 50% CA (30% T65)	534,76 +/- 33,85	291,00 +/- 15,98	836,80 +/- 39,16	2,88	1,021	0,7380
Ibuprofen-Na 70% CA (10% T65)	693,35 +/- 59,86	447,87 +/- 37,31	1020,56 +/- 70,82	2,28	0,826	0,7413
Ibuprofen-Na 70% CA (30% T65)	875,33 +/- 89,29	615,82 +/- 55,39	1195,15 +/- 151,65	1,94	0,662	0,7351

Table 12. Particle Size Distribution of samples and pure materials

***** SPAN is one of the common values for characterising the width of a particle size distribution and it is equal to:

$$SPAN = (X_{90}-X_{10})/X_{50}$$

Like in the case of the ratio X_{90}/X_{10}, the lower these values are, the narrower is the width of distribution.

From the table 12 it can be seen, that both for citric acid and Ibuprofen sodium dihydrate, the SPAN values clearly decrease and on the same time the aspect ratio increases. These results indicate a good coating quality and particles with narrower size distribution. In the case of NAc, the aspect ratio increases as well but the coating process leads to a slightly increased SPAN values, indicating that the coating process resulted in less homogenous coated particles than in the cases of the other two APIs.

On the other hand, despite of this increase on the width of the particle distribution, the absolute SPAN values of the coated NAc microcapsules are lower than the values of the rest APIs showing that despite of the less smooth coating process, the microcapsules produces possess a relative narrow width of particle size distribution. Also, even though the SPAN values slightly increase, the fact that the aspect ratio also increases is an indication that there is no agglomeration taking place during the procedure.

5.4 X-Ray diffraction

In order to investigate the crystallite thickness of the tristearin on the coatings of the microcapsules, the samples containing NAc where chosen both with 10% and 30% of Tween® 65.

The samples stored at room temperature and those at 40°C were compared in order to quantify any difference based on the storing conditions. For that reason, the small area of the x-ray diffraction pattern (SAXS) was analyzed. The diffraction patterns of the microcapsules consist of two visible diffraction peaks on the small angle area.

As an example, the microcapsules containing 70% of coating amount, of which 10% is Tween® 65 will be shown. The microcapsules stored at room temperature, showed a main reflection at the q vector positions of q_{001}=0.144 $Å^{-1}$ and one harmonic of this peak can also be observed at 3q=0.443 $Å^{-1}$. The sample stored at 40°C showed correspondingly a q_{001}=0.146 $Å^{-1}$ and 3q=0.447 $Å^{-1}$ (Fig. 52, 53).

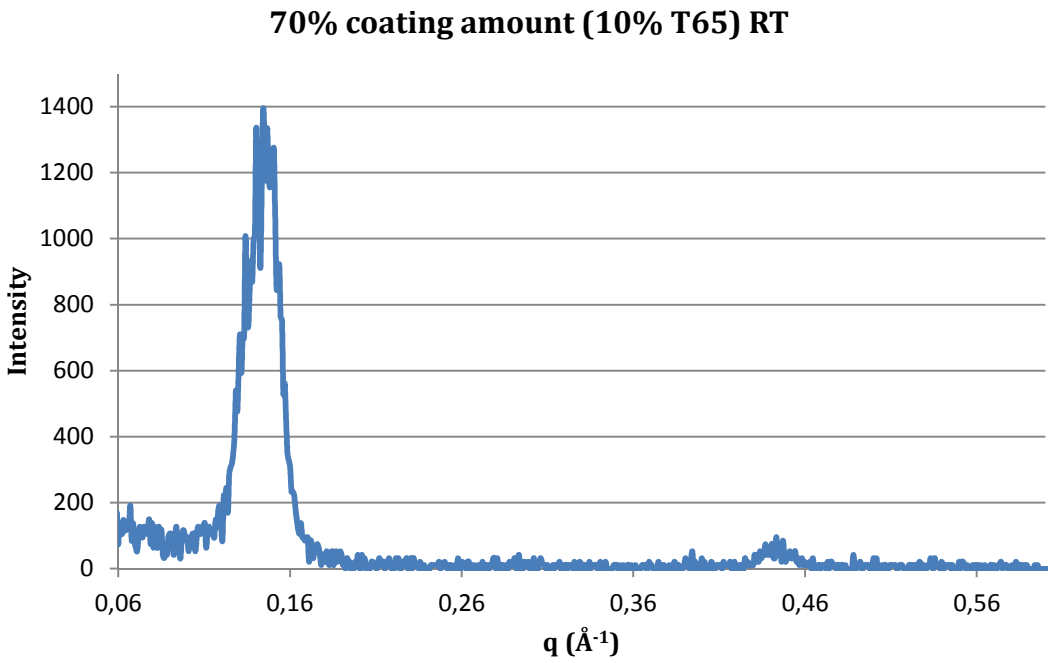

Figure 43. Diffraction peaks at room temperature

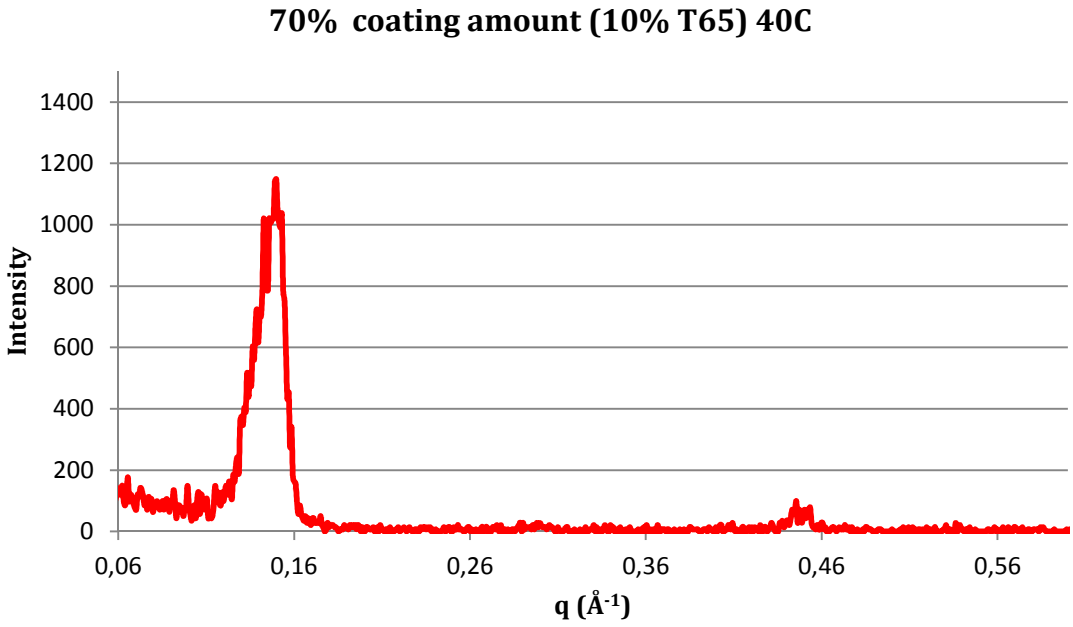

Figure 44. Diffraction peaks at 40°C

The corresponding lamellar thickness can be calculated either by using the main reflection or the harmonic. Given the fact that in our system there is always Tween® 65 present, using the main reflection would produce less accurate results, as the reflection peak of Tween® 65 is very close to the main reflection of the tripalmitin thus the actual merging of the two peaks causes imprecise results.

For that reason, the harmonic peak at 3q was used to calculate the lamellar thickness and this is done by using the equation $d=2\pi/3q$ and then multiplying the result with 3 because of using the 3q (harmonic) instead of the main reflection (q_{001}). The diffraction pattern of each sample was convolved with a Gaussian function using Matlab R2014a (MathWorks, Inc. Natick, Massachusetts)[32].

Using Matlab the resulted a, b and c parameters of the Gaussian function are taking into consideration for the further evaluation of the average crystallite thickness using the Sherrer equation:

$$D = \frac{K\lambda}{FWHMcos(\theta)}$$

Where FWHM = $2\sqrt{2\ln 2} \times c \approx 2{,}35482c$, λ=1,543Å, K=0,9 (good approximation), θ=b/2 as b indicates the position of the center of the peak which is equal to 2θ.

Applying the Sherrer formula for all the samples we end up with the following diagram comparing samples stored at room temperature and at 40°C. The y-axis (D in nm) indicates the thickness of the crystallite thickness in nanometers.

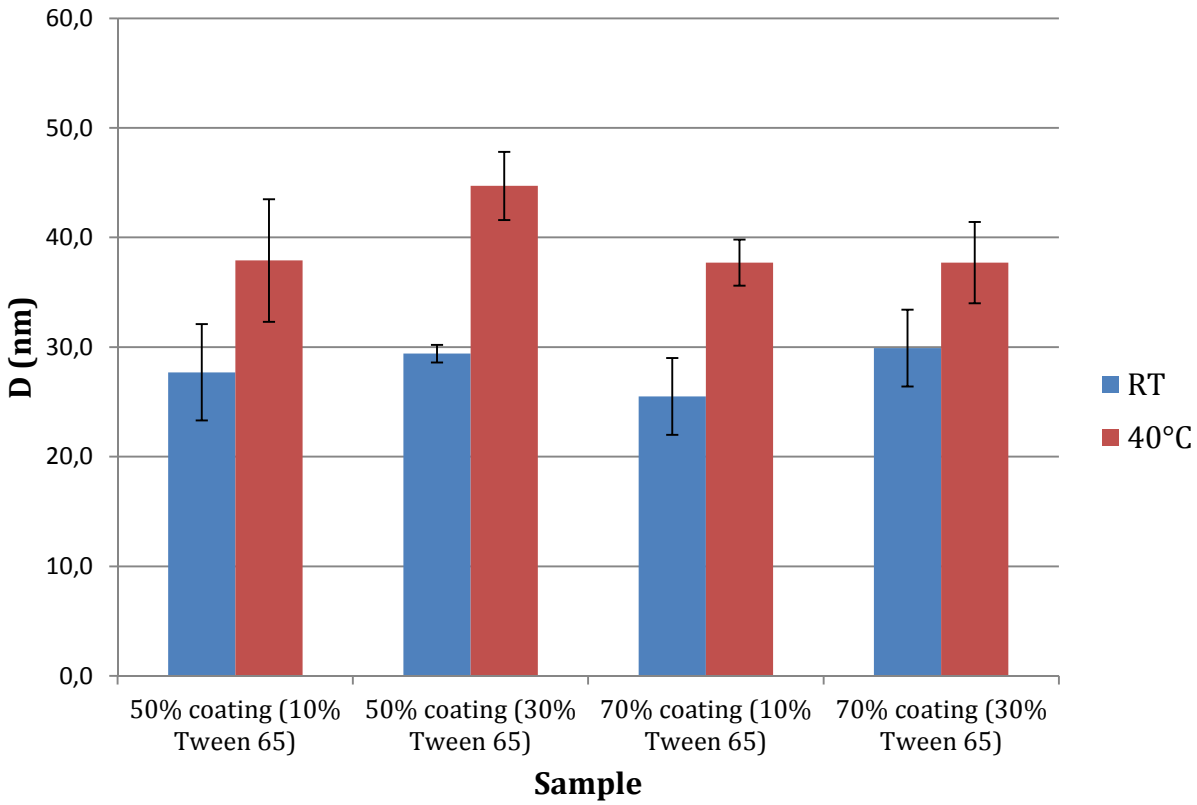

Figure 45. Crystallite thickness of the NAc containing microcapsules after storage at room temperature and at 40°C

6 DISCUSSION

The dissolution profiles of the tested microcapsules, showed a significant increase of the dissolution rate after storage at 40°C, particularly by having lower amounts of Tween® 65 in the system. This instability due to storage of formulations containing lipids as excipients has been observed in previous studies which include various theories explaining this phenomenon. A delayed release profile after storage of sustained release tablets containing an API and lipid excipient was explained based on hypothesis of either an altered distribution of the lipid component within the matrix structure or due to an alteration of the mesoscopic structure of the matrix [31]. In other studies an increased dissolution rate was observed which was explained based on the theory of transformation of the crystal form to more stable polymorphs upon storage [3,4].

In the present study however, the increase of the dissolution rate due to storage at elevated temperature cannot be explained with the theory of the polymorphic transformation due to the fact that the DSC results showed that with the addition already of 10% of Tween® 65 in the system, the unstable α-form disappears almost immediately (t0 results) in favor of the stable β-form of tripalmitin. After one month, even at room temperature, the α-form has transformed completely to β-form. This effect of Tween® 65-apart of aiding to the formulation in favor of a faster release acting as an emulsifier with a relative high HLB of 10,5- is known from previous studies where it is shown that after less than 4h at room temperature and with 10% of Tween® 65, the α-form completely disappears [6]. Reviews published evaluating the role of minor components and additives on lipids also point out in this direction [5,33] while older publication already mentioned the fact that depending on the emulsifier used, one or the other polymorphic form is favored [34].

The X-ray results showed a clear increase of the crystallite thickness by samples stored at 40°C as a response to increased temperature, thus a change of inner structure of the lipid/emulsifier coating. These data are in a well agreement with the DSC results showing the sharpening of the melting peak of beta form of tripalmitin and different mixtures of tripalmitin and Tween® 65 after storage. Of note, that this phenomenon could be observed after storage of all samples independent on the storage conditions.

In a recently published study [32] the same tendency has been observed on microcapsules containing tristearin as coating material and citric acid as API in the core.

All the tested samples yielded an average lamellae thickness of 4,2-4,3 nm. Although the DSC results indicate the presence of the lipid in the β-form, the lamellae thickness according to Kellens et al [8] lies between those of β' and β-form. These small differences could be due to the used SWAXS equipment, as previous studies clearly indicated that the lipid with the presence of even 10% of Tween® 65 exists in the β-form after less than 4 hours [6].

A novel explanation for this observed instability at 40°C could be based upon the following hypothesis;
As the DSC results among others confirmed, the surfactant in the coating layer is not microscopically miscible with the lipid and does not result in mono-phasic system, on the contrary both components co-exist separately. This was in some extend expected given the nature of Tween® 65 being a O/W emulsifier with a HLB of 10,5. This observation leads to the hypothesis that the coating is a dispersion, having Tween® 65 as the dispersed phase and tripalmitin as the continuous phase. When this formulation is kept at room temperature, the system is quite stable and it is a solid-solid dispersion.

When, however, the microcapsules are stored at 40°C this temperature is above the melting point of the emulsifier. Having the dispersed phase in a molten state the system is no longer a solid-solid but a liquid-solid dispersion. When the dispersed phase stays for a longer time in a molten state, the mobility of this phase is increased due to the thermodynamic conditions of storage at 40°C. The molecules of Tween® 65 merge with each other forming bigger channels. The tortuosity decreases thus the penetration of water inside creating an emulsion and cracks on the coating surface is easier. In a publication from Sugao et al [36] a similar behavior of the dissolution profile after heat-treating of the microparticles was observed however the emulsifier was not part of the coating originally but was used as a granulating excipient. Apart from that, the x-ray results showed that although the thickness of each lipid lamellae is constant, the thickness of the crystallites formed by these lamellas is increased. This is contributing to the fact that more space is created for the Tween® 65 as the lipid crystals also tend to merge and grow in size creating ticker crystallites. In other words, a two-phasic system

tends to separate in favor of lower inner energy. A rough schematical representation can be seen in the Figure 55.

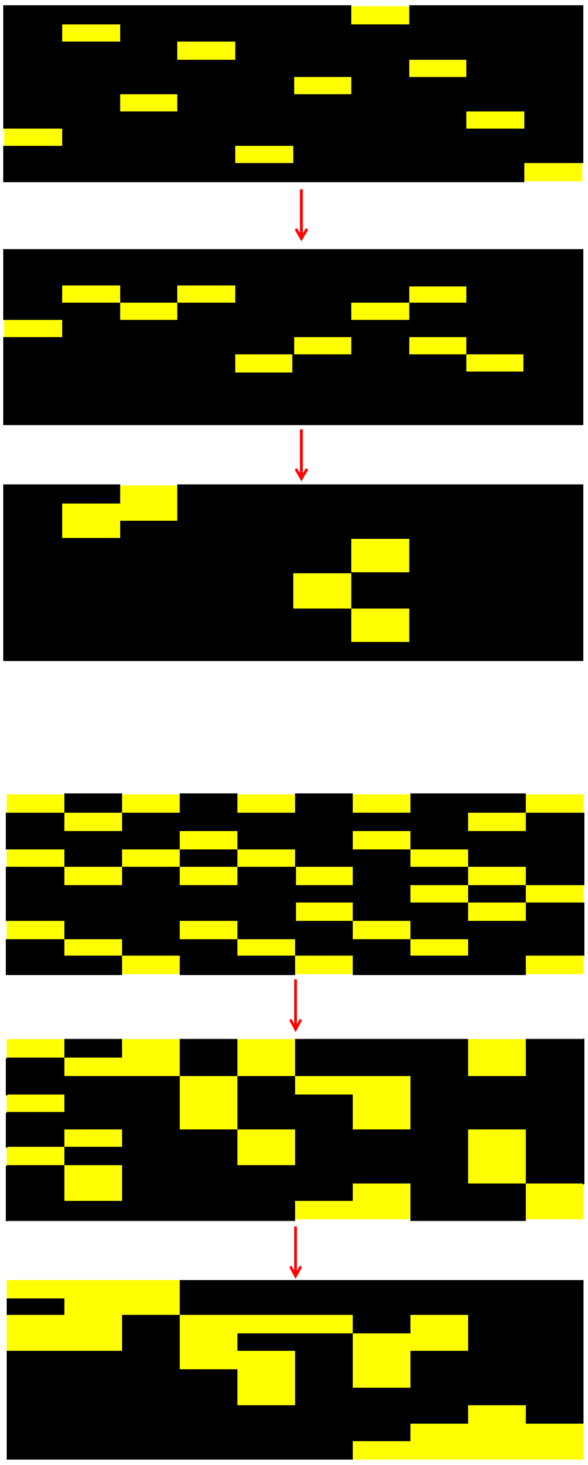

Figure 46. Schematic representation of the hypothesis

In these sketches, the yellow color indicates the Tween® 65 and the black color the lipid crystallites. The first sketch represents the coatings with 10% emulsifier and the second the coatings with 30% emulsifier, where the hypothesis is easier observed.

7 CONCLUSION

The present study investigated the stability of microcapsules produced with the hot-melt coating technique. As coating formulation, different blends of a lipid excipient (tripalmitin) and an emulsifier (Tween® 65) were used.

The dissolution profiles that were investigated after production as well as after storage for one and three months under room temperature and at 40°C indicated that the samples stored at elevated temperature showed an accelerated dissolution profile after storage.

In order to further investigate the reasons for such a phenomenon, differential scanning calorimetry (DSC) and X-ray diffraction techniques were applied.

The results of the DSC indicate the separate presence of the emulsifier even at the lowest concentrations, which could be used as an indication that the emulsifier and the lipid are forming a type of dispersion. This theory is also based on the fact that the emulsifier used (Tween® 65) is a relative hydrophile emulsifier with an HLB of 10,5 thus its solubility in the lipid component is very low.

The results of the X-ray diffraction clearly showed a growth of the crystallites size of the lipid component when samples are stored at 40°C in comparison to the ones stored at room temperature.

These indications lead to the hypothesis that the dispersion that is formed from the two components undergoes a change when the samples are stored at 40°C. At this temperature, one component –the emulsifier- is at molten state thus the solid-solid suspension changes to a solid-liquid type. The liquid molecules of the emulsifier are more mobile and they merge, forming bigger channels allowing water to penetrate easier the structure thus leading to a faster dissolution profile. This phenomenon is

enhanced from the fact that the lipid crystals are also merging and growing in size, allowing more space for the emulsifier to form bigger channels.

8 BIBLIOGRAPHY

[1] S. Srivastava, G. Mishra, Fluid Bed Technology : Overview and Parameters for Process Selection, Int. J. Pharm. Sci. Drug Res. 2 (2010) 236–246.

[2] S.G. Sudke, D.M. Sakarakar, Lipids - An instrumental excipient in pharmaceutical hot-melt coating, Int. J. PharmTech Res. 5 (2013) 607–621.

[3] Y.W. Choy, N. Khan, K.H. Yuen, Significance of lipid matrix aging on in vitro release and in vivo bioavailability, Int. J. Pharm. 299 (2005) 55–64. doi:10.1016/j.ijpharm.2005.04.030.

[4] N. Khan, D.Q.M. Craig, Role of blooming in determining the storage stability of lipid-based dosage forms, J. Pharm. Sci. 93 (2004) 2962–2971. doi:10.1002/jps.20210.

[5] K. Sato, L. Bayés-García, T. Calvet, M.À. Cuevas-Diarte, S. Ueno, External factors affecting polymorphic crystallization of lipids, Eur. J. Lipid Sci. Technol. 115 (2013) 1224–1238. doi:10.1002/ejlt.201300049.

[6] K. Becker, Advanced stable lipid-based formulations for a patient-centric product design, (2015).

[7] C. Himawan, V.M. Starov, a. G.F. Stapley, Thermodynamic and kinetic aspects of fat crystallization, Adv. Colloid Interface Sci. 122 (2006) 3–33. doi:10.1016/j.cis.2006.06.016.

[8] M. Kellens, W. Meeussen, H. Reynaers, Crystallization and phase transition studies of tripalmitin, Chem. Phys. Lipids. 55 (1990) 163–178. doi:10.1016/0009-3084(90)90077-5.

[9] S. Metin, R. Hartlel, Crystallization of Fats and Oils, Bailey's Ind. Oil Fat Prod. (2005). doi:10.1002/047167849X.bio021.

[10] K. Sato, Crystallization behaviour of fats and lipids — a review, Chem. Eng. Sci. 56 (2001) 2255–2265. doi:10.1016/S0009-2509(00)00458-9.

[11] S.H.J. Idziak, Powder X-Ray diffraction of triglycerides in the study of polymorphism, in: A.G. Marangoni (Ed.), Struct. Anal. Edible Fats, 2012.

[12] F. Lavigne, C. Bourgaux, M. Ollivon, Phase transitions of saturated triglycerides, J. Phys. IV. 3 (1993) 137–140. doi:10.1051/jp4:1993825.

[13] V. Jannin, Y. Cuppok, Hot-melt coating with lipid excipients, Int. J. Pharm. 457 (2013) 480–487. doi:10.1016/j.ijpharm.2012.10.026.

[14] W.-C. Yang, HANDBOOK of FLUIDIZfiTION and FLUID-PARTICLE SYSTEMS, 2003.

[15] K. Christoph Link, E.-U. Schlünder, Fluidized bed spray granulation, Chem. Eng. Process. Process Intensif. 36 (1997) 443–457. doi:10.1016/S0255-2701(97)00022-6.

[16] D.M. Parikh, Handbook of Pharmaceutical Granulation Technology, (1997) 532. doi:10.1201/9780849354953.ch17.

[17] S. Dhuppe, Recent Techniques of pharmaceutical solventless coating: a review, Int. J. Pharm. Sci. Res. 3 (2012) 1976–1986.

[18] S.G. Sudke, D.M. Sakarakar, Hot-melt coating: An innovative pharmaceutical coating technique, J. Pharm. Res. Clin. Pract. 3 (2013) 16–26.

[19] D.Q.M. Craig, M. Reading, Thermal Analysis of Pharmaceuticals, 1st ed., 2006.

[20] A.G. Marangoni, Stucture-Function Analysis of Edible Fats, 1st ed., 2012.

[21] C.M. Clark, B.L. Dutrow, Single-crystal X-Ray Diffraction, (2015). http://serc.carleton.edu/research_education/geochemsheets/techniques/SXD.html (accessed July 20, 2015).

[22] R.A. Harvey, P.C. Champe, Pharmacology, 2005.

[23] Ph. Eur. 6.0 - Acetylcysteine, (2008) 1100–1101. http://www.uspbpep.com/ep60/acetylcysteine 0967e.pdf (accessed July 28, 2015).

[24] DrugBank, DrugBank - Acetylcysteine, (2008). http://www.drugbank.ca/drugs/db06151 (accessed August 4, 2015).

[25] BASF, BASF - Ibuprofen sodium dihydrate, (2008). http://www.pharma-ingredients.basf.com/ (accessed July 16, 2015).

[26] Ph. Eur. 6.0 - Ibuprofen, (2008) 2119–2121. http://www.uspbpep.com/ep60/ibuprofen 0721e.pdf (accessed August 5, 2015).

[27] H. Ammon, C. Hunnius, Hunnius Pharmazeutisches Wörterbuch, 2004.

[28] F. Massholder, Polysorbat 65 - Lebensmittellexikon, (2014). http://www.lebensmittellexikon.de/p0002340.php (accessed July 30, 2015).

[29] A. Gadhave, Determination of Hydrophilic-Lipophilic Balance Value, 3 (2014) 573–575.

[30] S.S. Behzadi, S. Toegel, H. Viernstein, Innovations in coating technology., Recent Pat. Drug Deliv. Formul. 2 (2008) 209–230. doi:10.2174/187221108786241633.

[31] V. Jannin, Y. Rosiaux, J. Doucet, Exploring the possible relationship between the drug release of Compritol®-containing tablets and its polymorph forms using micro X-ray diffraction, J. Control. Release. 197 (2015) 158–164. doi:10.1016/j.jconrel.2014.11.013.

[32] D.G. Lopes, K. Becker, M. Stehr, D. Lochmann, D. Haack, A. Zimmer, et al., Role of Lipid Blooming

and Crystallite Size in the Performance of Highly Soluble Drug-Loaded Microcapsules, J. Pharm. Sci. (2015) n/a–n/a. doi:10.1002/jps.24660.

[33] K.W. Smith, K. Bhaggan, G. Talbot, K.F. Van Malssen, Crystallization of fats: Influence of minor components and additives, JAOCS, J. Am. Oil Chem. Soc. 88 (2011) 1085–1101. doi:10.1007/s11746-011-1819-7.

[34] N. Garti, J. Schlichter, S. Sarig, DSC Studies Concerning Polymorphism of Saturated Monoacid Triglycerides in the Presence of Food Emulsifiers, Fett Wiss. Technol. Sci. Technol. 90 (1988) 295–299. doi:10.1002/lipi.19880900803.

[35] P. Elisabettini, A. Desmedt, V. Gibon, F. Durant, Effect of Sorbitan Tristearate on the Thermal and Structural Properties of Monoacid Triglycerides: Influence of a “Cis” or “Trans” Double Bond, (1995) 65–69. doi:DOI: 10.1002/lipi.19950970206.

[36] H. Sugao, S. Yamazaki, H. Shiozawa, K. Yano, Taste masking of bitter drug powder without loss of bioavailability by heat treatment of wax-coated microparticles, J. Pharm. Sci. 87 (1998) 96–100. doi:10.1021/js970104g.

[37] Stearic acid, Wikipedia. (2007). www.wikipremed.com (accessed June 30, 2015).

[38] Tripalmitin basic information, (2008). www.chemicalbook.com/ProductChemicalPropertiesCB9163652_EN.htm (accessed July 2, 2015).

[39] Tristearin basic information, (2010). http://www.chemicalbook.com/ChemicalProductProperty_EN_CB9110090.htm (accessed August 13, 2015).

[40] B. Papankova, Laboratory of calorimetry-DSC, (2012). http://www.fchpt.stuba.sk/sk/ustavy-a-oddelenia/ustav-anorganickej-chemie-technologie-a-materialov/oddelenie-anorganickej-chemie/laboratoria/laboratorium-kalorimetrie.html?page_id=2890 (accessed September 2, 2015).

[41] DrugBank, DrugBank - Citric acid, (2005). http://www.drugbank.ca/drugs/DB04272 (accessed July 23, 2015).

[42] Tripalmitin structure, NIST. (2011). http://webbook.nist.gov/cgi/cbook.cgi?ID=555-44-2 (accessed July 23, 2015).

[43] Polysorbat 65, Wikipedia. (2015). https://de.wikipedia.org/wiki/Polysorbat_65 (accessed July 25, 2015).

9 APPENDIX

Table of figures

Tables

List of abbreviations

API: Active Pharmaceutical Ingredient

DSC: Differential Scanning Calorimetry

IUPAC: International Union of Pure and Applied Chemistry

NAc: N-Acetylcysteine

NAPQI: N-acetyl-p-benzoquinone imine

RT: Room Temperature

TAG: Triacylglycerol

SAXS: Small Angle X-ray Scattering

WAXS: Wide Angle X-ray Scattering